universität wien

MASTERARBEIT / MASTER'S THESIS

Titel der Masterarbeit / Title of the Master's Thesis

„Establishment and optimization of the radiosyntheses of Gallium-68 labeled compounds using microwave and microfluidic devices. "

verfasst von / submitted by

Erwin Schaier, BSc

angestrebter akademischer Grad / in partial fulfilment of the requirements for the degree of

Master of Science (MSc)

Wien, 2020 / Vienna 2020

Studienkennzahl lt. Studienblatt / degree programme code as it appears on the student record sheet:	UA 066 862
Studienrichtung lt. Studienblatt / degree programme as it appears on the student record sheet:	Masterstudium Chemie
Betreut von / Supervisor:	Assoc. Prof. Priv.-Doz. Mag. Dr. Wolfgang Wadsak

„Es ist noch nicht genug, eine Sache zu beweisen, man muß die Menschen zu ihr auch noch verführen oder zu ihr erheben.“

- Friedrich Wilhelm Nietzsche

Acknowledgments

First of all, I want to thank my supervisor Wolfgang Wadsak for the introduction into the interesting field of radiochemistry und nuclear medicine. His support for my academic development and beyond is immeasurable. His ear was always open for any issue, academically or otherwise.

I want to thank Sarah Pfaff for her patience and tutelage. Her willingness for critique, when it was needed and advice were essential for the completion of this thesis. I wish her all the best in her further career.

I also want to thank my other colleagues during my time in the radiochemistry group, especially Chrysoula Vraka, for their helpfulness and good teamwork.

My eternal gratitude belongs to my family and friends for laying the foundation on which my life is built.

Finally, I want to thank Neptun Yousefi for always telling me to keep my head up and making every day a bit brighter.

Abstract

The role of positron emission tomography (PET) as an imaging tool for physiological and pathological processes has increased drastically over the last years. A main application of this noninvasive technique is the diagnosis of tumors and their metastases. Among the commonly used PET nuclides gallium-68 has become increasingly attractive for radiolabeling due to its advantageous half-life and good availability of this nuclide. The latter is facilitated by the ^{68}Ge/^{68}Ga-generator system, in contrast to other PET nuclides produced by a cyclotron. With the recent development of several ^{68}Ga-labeled radiotracers and their following clinical use, the availability of different synthesizing devices to obtain higher radiochemical yields within a short time has become a topic of interest. Among these techniques, microwave-assisted complexation and radiolabeling using a microfluidic system could be promising methods for clinical routine.

Microwave irradiation has several advantages over regular heating methods such as a highly time-efficient heating and minimal temperature gradients within the reaction solution. Microwave assisted synthesis can result in remarkably high yields or enables syntheses, which are usually not feasible using conventional heating methods.

The microfluidic approach using a flow through reactor allows an increased conversion rate due to a high surface to volume ratio and the heating over the boiling point of the solvent. Furthermore, microfluidic modalities may offer the production of radiotracers according to a dose on demand concept.

The scope of this master thesis includes the microwave-assisted synthesis of [^{68}Ga]Ga-PSMA-11, [^{68}Ga]Ga-DOTA-NOC and [^{68}Ga]Ga-NODAGA-RGDyk. For this purpose, these gallium-68 radiotracers were produced by variation of different reaction parameters like precursor concentration and applied power. These parameters were optimized as far as possible. As a result, outstanding conversion rates have been achieved using minimal precursor amounts, especially for [^{68}Ga]Ga-PSMA-11 and [^{68}Ga]Ga-NODAGA-RGDyk.

Additionally, PSMA-11 and NODAGA-RGDyk were ^{68}Ga-labeled using a microfluidic flow-through reactor. Here excellent conversion rates were achieved as well. Hence, both methods are useful options for special or routine demands in radiolabeling with gallium-68.

Zusammenfassung

Die Bedeutung der Positronen-Emissions-Tomographie (PET) als Bildgebungsmethode für physiologische und pathologische Prozesse ist drastisch über die letzten Jahre gestiegen. Eine Hauptanwendung dieser nicht-invasiven Methode ist die Diagnose von Tumoren und deren Metastasen. Unter den häufig verwendeten PET-Nukliden ist Gallium-68 aufgrund seiner vorteilhaften Halbwertszeit und guten Verfügbarkeit zunehmend attraktiv geworden. Letztere ist durch das ^{68}Ge/^{68}Ga-Generator-System möglich, welche, im Gegensatz zu anderen PET-Nukliden, durch ein Zyklotron produziert werden. Mit der neuesten Entwicklung einiger ^{68}Ga-markierten Radiotracer und ihrer klinischen Anwendung ist die Nutzbarkeit verschiedener Synthese-Geräte von Interesse, um höhere radiochemische Ausbeuten in kurzer Zeit zu erzielen. Unter diesen Methoden scheint die Radiomarkierung durch ein Mikrowellen- oder ein mikrofluides System vielversprechend für den klinischen Alltag zu sein.

Bestrahlung mit Mikrowellen weist einige Vorsteile gegenüber konventionellen Heizmethoden auf, wie z.B. die hohe Zeiteffizienz oder minimale Temperaturgradienten innerhalb der Reaktionslösung. Mikrowellen-unterstützte Synthese kann bemerkenswert hohe Ausbeuten erreichen oder Synthesen erlauben, welche für gewöhnlich mit herkömmlichen Heizmethoden oft nicht realisierbar sind.

Der mikrofluide Ansatz mittels eines Durchfluss-Reaktors erlaubt hohe Konversionsraten durch ein hohes Oberflächen- zu Volumenverhältnis und das Erhitzen über den Siedepunkt. Ferner könnten mikrofluide Ansätze die Möglichkeit für ein „dose-on-demand“-Konzept bieten, bei welchem genau definierte Aktivitäten auf Abruf produziert werden können.

Diese Masterarbeit umfasst die Synthese von [^{68}Ga]Ga-PSMA-11, [^{68}Ga]Ga-DOTA-NOC und [^{68}Ga]Ga-NODAGA-RGDyk mit einer PET-Labormikrowelle. Hierzu wurden diese ^{68}Ga-Radiotracer unter Variation verschiedener Reaktionsparameter, wie Precursor-Konzentration, Temperatur und Mikrowellenleistung hergestellt. Diese Parameter wurden soweit möglich optimiert. Hierbei konnten herausragende Umsatzraten unter der Verwendung geringster Precursor-Mengen vor Allem für [^{68}Ga]Ga-PSMA-11 und [^{68}Ga]Ga-NODAGA-RGDyk erzielt werden.

Zusätzlich wurden PSMA-11 und NODAGA-RGDyk über einen mikrofluiden „flow-through“ Reaktor ^{68}Ga-markiert. Auch hier konnten exzellente Umsatzraten erzielt werden. Folglich sind beide Methoden nützliche Optionen für Spezial- oder Routineanforderungen in der Radionuklidmarkierung mit Gallium-68.

Table of Content

I. Introduction 1

Imaging techniques in medicine 1

Positron Emission Tomography (PET) 2

Principles of radiotracers 3

Chemical properties of gallium 6

Principles of generator systems 6

History and development of ^{68}Ge/^{68}Ga-generators 8

Microwave assisted synthesis 9

Microfluidic devices in radiosynthesis 13

Targeting the SST-receptors *via* [^{68}Ga]Ga-DOTA-NOC 15

Targeting PSMA *via* [^{68}Ga]Ga-PSMA-11 16

Targeting the $\alpha_v\beta_3$ receptor *via* [^{68}Ga]Ga-NODAGA-RGD 18

II. Aim 20

III. Materials and Methods 21

Materials 21

Methods 21

General procedure for radiosynthesis using a microwave module 22

General procedure for radiosynthesis using a microfluidic device 22

Quality control 23

IV. Results and Discussion 26

Microwave-assisted radiosynthesis of [^{68}Ga]Ga-DOTA-NOC 26

Influence of precursor concentration on [^{68}Ga]Ga-DOTA-NOC microwave synthesis 26

Influence of temperature on [^{68}Ga]Ga-DOTA-NOC microwave synthesis 28

Influence of power on [^{68}Ga]Ga-DOTA-NOC microwave synthesis 30

Evaluation of [^{68}Ga]Ga-DOTA-NOC microwave synthesis 31

Microwave-assisted radiosynthesis of [^{68}Ga]Ga-PSMA-11 32

Influence of precursor concentration on [^{68}Ga]Ga-PSMA-11 microwave synthesis 32

Influence of temperature on [^{68}Ga]Ga-PSMA-11 microwave synthesis 32

Influence of power on [^{68}Ga]Ga-PSMA-11 microwave synthesis 33

Evaluation of [^{68}Ga]Ga-PSMA-11 microwave synthesis 34

Microwave-assisted radiosynthesis of [^{68}Ga]Ga-NODAGA-RGDyk 35
Influence of precursor concentration on [^{68}Ga]Ga-NODAGA-RGDyk microwave synthesis 35
Influence of temperature on [^{68}Ga]Ga-NODAGA-RGDyk microwave synthesis 35
Influence of power on [^{68}Ga]Ga-NODAGA-RGDyk microwave synthesis 36
Evaluation of [^{68}Ga]Ga-NODAGA-RGDyk microwave synthesis 37
Influence of buffer choice on microwave synthesis of ^{68}Ga-radiotracers 38
Microfluidic device-assisted radiosynthesis of ^{68}Ga-labeled tracers 41
Influence of precursor concentration on microfluidic synthesis of [^{68}Ga]Ga-PSMA-11 41
Influence of temperature on microfluidic synthesis of [^{68}Ga]Ga-PSMA-11 42
Influence of temperature on microfluidic synthesis of [^{68}Ga]Ga-NODAGA-RGDyk 42
Comparison between Microwave- and Microfluidic-assisted ^{68}Ga-labeling 44
V. Conclusion and Outlook 45
VI. Abbreviations 47
VII. Figure Caption 48
VIII. References 50

I. Introduction

Imaging techniques in medicine

Imaging techniques utilizing radiotracers differ from regular imaging methods in the type of obtained information: X-ray, CT and MRI show morphological information, while nuclear imaging methods visualize physiological processes. While the formers are crucial for the investigation of pathologies with clear morphological changes and are more broadly providable, imaging in nuclear medicine can be targeted towards specific functional abnormalities or small morphological changes (e.g. tumor lesions), which often are manifested before any substantial morphological changes occur. This decreases the necessary time for a diagnosis immensely.

Radiochemistry and Nuclear Medicine

Radiochemistry studies the reactions of molecules with naturally occurring as well as artificial radioactive isotopes. This includes the synthesis of novel radioactive compounds as well as the investigation of processes with ionizing radiation as a very sensitive marker and means of detection. Radioactive isotopes do not differentiate themselves from their stable counterparts in their physicochemical properties (for almost all cases) and decay with diverse modes of emissions. The main natural modes of decay are alpha- (emission of a helium nucleus), beta minus- (conversion of a neutron into a proton and an accelerated electron) and gamma radiation (emission of high energy photons by relaxation of an excited nucleus). Artificially produced radionuclides may decay in other modes as well, such as beta plus decay (transmutation of a proton into a neutron and a positron).[1] Those artificial nuclides are produced either by reactor, generator or accelerator, each associated with varying expenditures. Radiochemical applications include the study of chemical reaction mechanisms, classic DNA sequencing[2], dating of inorganic and organic materials by measurement of radioactive traces (e.g. environmental studies)[3] and the large field of nuclear medicine.

Nuclear medicine utilizes the knowledge and technologies of radiochemistry to form a specialty within medicine with unique techniques for diagnosis and the treatment of diseases. The special features in the diagnostic modalities of nuclear medicine, positron emission tomography (PET) and single photon emission computed tomography (SPECT) are the visualization of physiological processes rather than morphological ones. The interpretation can be drastically aided by using hybrid modalities like SPECT-CT, PET-CT or PET-MRI. Therapeutic interventions in nuclear medicine are either anatomically or physiologically targeted and require the administration of radiotracers.

Positron Emission Tomography (PET)

In positron emission tomography, radiotracers are usually administered intravenously. This technique is featured by beta plus decaying nuclides which are utilized for their positron emission. After the PET tracer is administered, it accumulates in its target region. The emitted positron themselves are not detected, but rather the resulting annihilation radiation of two gamma photons with an energy of 511 keV, which are emitted in opposite direction (line of response) after the collision of the positron with an electron. After administration, the patient passes through the circular axis of a detector ring and the gamma photons are registered on opposing sites of the detector. Consequently, the position of the annihilation event along the line of response can be reconstructed. These solid scintillation detectors can be based on different types of crystals (sodium iodine NaI, *GSO* gadolinium oxyorthosilicate (Gd_2SiO_5:Zr), LYSO lutetium yttrium oxyorthosilicate ($LuYSiO_5$:Ce), $LaBr_3$ lanthanum bromide) and are linked to a photomultiplier tube and a pulse height analyzer, which can distinguish coinciding decay photons from scattered ones by the level of their respective energy. This signifies a huge advantage for PET over SPECT in sensitivity, since only coinciding detection events within a short time frame of approximately 10 nanoseconds are registered as a decay signal, thus avoiding the signals of random coincidences from scattering and therefore eliminating the need for an aperture in the form of a lead collimator.[4]

PET/CT fusion imaging technique distinguishes itself through high sensitivity, specificity and accuracy in tumor detection due to its combination of morphological data (CT) and physiological information (PET). The consecutive recording of both CT and PET data allows the accurate alignment of both images and attenuation correction of the positron emission. PET/CT is the gold standard for the exploration and observation of malignancies in oncology.[4] Although not as commonly available, the combination of PET and MRI provides advantages in the investigation of diseases, where enhanced soft tissue contrast is of diagnostic value und the reduction of radiation dose is of clinical concern (e.g. children or patients with successive scans).[5]

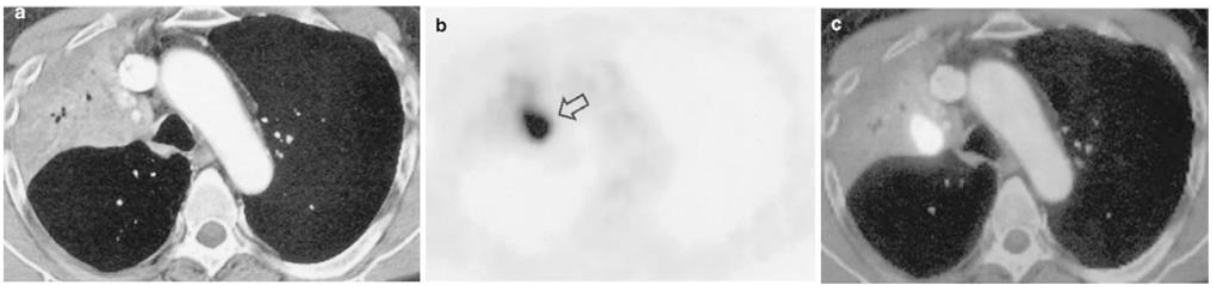

Figure 1: Transverse (a) CT, (b) PET, and (c) PET/CT fused images of a thorax with non-small cell lung carcinoma ([^{18}F]FDG.)[6]

A wide variety of PET tracers and applications have been developed for several pathological disorders utilizing different positron emitters.

Principles of radiotracers

Radiopharmaceuticals are radiolabeled compounds, developed for *in vivo* applications in patients, either for diagnostic or therapeutic purposes. By principle, most radiotracers contain two crucial elements; an appropriate radionuclide for the intended application and a specific molecular structure, which acts as a vector to the target. Frequently, those elements need to be connected by a linking structure (e.g. a chelator for radiometals). Possible targets include antigens, receptors, enzymes and transporters, whose physiological and pathophysiological processes and functions can be visualized through this approach.

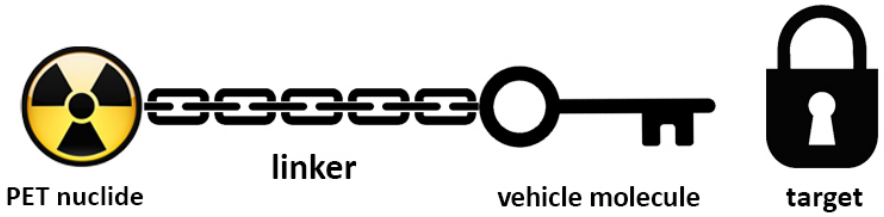

Figure 2: Structural elements of a PET radiotracer (adapted from [7])

The vector structure of the tracer has the task to facilitate the transport of the radiation source to the specific target site. These imaging methods allow the investigation of manifold functions like metabolic changes, protein expression and perfusion. For this purpose, the vehicle molecule acts as an agonist or antagonist for a receptor or as a substrate for an enzyme or transporter, often mimicking the structure of physiological molecules. Resultantly, biomolecules can be labeled with a radioactive nuclide by isotopic substitution: An atom is exchanged with its radioactive isotope. Hence, the molecular structure stays the same and physicochemical properties, biodistribution and pharmacokinetic of the radiolabeled compound is not altered. In this light, naturally occurring carbon or oxygen are displaced with β^+-emitting carbon-11 or oxygen-15. The drawback of those nuclides is their short half-life (carbon-11: 20 min, oxygen-15: 2 min) that is associated with a challenging synthesis design. Consequentially, biomolecules can be labeled *via* non-isotopic substitution like radiofluorinations. Non-isotopic substitution causes a difference in the molecular structure, which can be beneficial or disadvantageous for pharmacodynamical and -kinetical behavior of the compound. In some instances, this effect is even proven to be useful for imaging (e.g. glucose trapping of [^{18}F]FDG).[8] In the case of radiometals, the nuclide cannot be incorporated directly into the vehicle molecule but

has to be connected by a chelator with an additional linking structure (e.g. DOTA as a chelator for gallium-68 or lutetium-177).

The radioactive isotopes for radiolabeling are chosen dependent on the intended task, since the needed radiophysical characteristics can vary substantially. For diagnosis, radiation with a high penetration depth for biological tissue is necessary, as the detection occurs outside the patient. Additionally, the half-life of the radionuclide should be short to reduce unnecessary radiation exposure to the patient and the staff, but still long enough to allow the radiolabeling process and imaging procedure with enough leftover activity after accumulation at the target side. On the other hand, the use of therapy tracers (mostly used for malignant diseases) demands different properties of their nuclides. Since the malignant tissue is to be damaged by the ionizing radiation, the exposure to it should be supported by a relatively long half-life of the nuclide, but also not extensively long due to inevitable damage to healthy tissue. Also, the type of radiation plays an important role in the effectiveness of the therapeutic tracer. Hence, isotopes with high radiation energy and low penetration depth radiation (beta-, alpha- and Auger electron radiation) are applied for localized radiation therapy of tumors. If the radiolabeling of a tracer is feasible with a diagnostic as well as a therapeutic nuclide, a theranostic approach might be applicable (e.g. [^{68}Ga]Ga-PSMA-11 and [^{177}Lu]Lu-PSMA). While the therapeutic radiotracer ([^{177}Lu]Lu-PSMA) is treating the disease, the diagnostic radiotracer enables the initial diagnosis and observing of therapeutic response. [9]

Radionuclide	Half-life	E_{max} [keV]	Mode of decay	Production
PET nuclides				
^{11}C	20.39 min	961	β^+ (100%)	Accelerator
^{13}N	9.97 min	1190	β^+ (100%)	Accelerator
^{15}O	2.04 min	1732	β^+ (100%)	Accelerator
^{18}F	109.77 min	634	β^+ (97%)	Accelerator
^{68}Ga	67.63 min	1899; 770	β^+ (89%)	Generator
SPECT nuclides				
^{99m}Tc	6.01 h	141	γ	Generator
^{123}I	13.22 h	159	γ	Accelerator
Therapeutic radionuclides				
^{90}Y	64.10 h	2270	β^-	Generator
^{131}I	8.02 d	1810	β^-	Fission
^{153}Sm	1.95 d	103 (280)	γ (β^-)	Reactor
^{177}Lu	6.71 d	113, 208.4 (598)	γ (β^-)	Reactor
^{186}Re	3.72 d	1100	β^-	Reactor

Figure 3: Commonly used radionuclides in nuclear medicine (adapted from [10])

Over the years, a huge variety of PET tracers have been developed, which feature radionuclides like carbon-11, nitrogen-13, oxygen-15, fluorine-18 and gallium-68. Fluorine-18 is the most preferred due to its relatively long half-life of 110 minutes, apparent through the high frequency of [^{18}F]FDG syntheses in clinical routine. However, clinical study applications of PET radiotracers are manifold and range from the detection of various tumors ([^{18}F]FDG, [^{11}C]MET, [^{68}Ga]Ga-DOTA-TOC)[11], functional brain imaging of multiple sclerosis([^{18}F]FDG, [^{11}C]PK11195)[12], epilepsy ([^{11}C]flumazenil, [^{18}F]MPPF, [^{11}C]cerfentanil)[13], depression ([^{11}C]raclopride, [^{11}C]5-hydroxytryptophan)[14] to the investigation of myocardial perfusion ([^{15}O]H_2O, [^{82}Rb]Rb).[15]

Chemical properties of gallium

Gallium is a post-transitional metal with an electron configuration of [Ar] 3d10 4s2 4p1. Hence, it is predominately found in the oxidation state +III, since the formed complexes in that state are stabilized by the d10 electron configuration. In acidic aqueous solutions, gallium(III) salts form the hydrated gallium ion, $[Ga(H_2O)_6]^{3+}$. At a pH = 5.1 it starts to precipitate as $Ga(OH)_3$, which can be dissolved as the $Ga(OH)_4^-$ anion at pH = 9.6 and higher.[16,17] Ga^{3+} is a hard Lewis acid and thus forms complexes with donor moieties like carboxylates and amines.[18] A distorted octahedral geometry is preferred with a coordination number of six.[19] Due to the protonation of donor groups at low pH, a pH range of 3.5 – 5.1 is necessary for Ga-complexation and thus the solution require buffering, accordingly. With a very similar ion radius as high spin Fe(III) (0.62 Å for Ga(III) and 0.65 Å for high spin Fe(III)), Ga(III) high spin Fe(III) both have similar chemical properties. This also partially explains the biodistribution of Ga.[20] Therefore, a strict avoidance of Fe(III) is necessary for successful Ga-labeling (e.g. no use of syringes made out of steel). As a transitional metal, gallium cannot form covalent bonds with the carbon-frame of a tracer molecule. Therefore, a chelating agent is necessary as a linkage.

Principles of generator systems

Due to the short half-life of many PET nuclides and the huge instrumental effort related to reactors, a method with good availability to produce PET nuclides is in high demand for clinical applications. A generator system is an alternative for production of short-lived radionuclide production. It is based on a pair of parent and daughter-radionuclide, where the short-lived daughter nuclide is formed by the long-lived parent-nuclide and can be extracted afterwards. The parent nuclide is fixed to a stationary matrix, whereas the daughter nuclide will differ in their physicochemical properties and can be separated *via* elution. Afterwards, the activity of the daughter nuclide must recover within a certain period as it is continuously restored by the decaying parent nuclide, as described by the Bateman equation, formulating this equilibrium:

$$A_d(t) = \left\{\left[A_p(0)\frac{\lambda_d}{\lambda_d - \lambda_p} * (e^{-\lambda_p t} - e^{-\lambda_d t}\right] * B.R.\right\} + A_d(0)e^{-\lambda_t}$$

Figure 4: Bateman equation for the determination of the daughter activity Ad(t)[21]

The daughter nuclide activity $A_d(t)$ at the time *t* is determined by the parent nuclide activity $A_p(t)$ and their respective decay constants λ_d and λ_p (B.R. is the branching ratio of the decay products of the parent nuclide, if more than the daughter nuclide of interest can be formed). However, the obtained activity is for most generators is 80 to 90% of the expected activity of the daughter nuclide by calculation. Several factors may attribute to this effect like size of the column, the used eluent volume

and chemical changes within the matrix due to high levels of radiation.[22] For generators of daughter-nuclides with longer half-life like ^{99m}Tc, residual activity can add up to the new starting activity A_0 for the following elution:

$$Y_2 = \frac{Y_1 * (e^{-\lambda_p \Delta t_2} - e^{-\lambda_d \Delta t_2})}{\left[1 - e^{-(\lambda_d - \lambda_p)\Delta t_1}\right]}$$

Figure 5: Equation for a starting activity after incomplete elution in a generator system[21]

Y_2 is the calculated yield of the current elution, following the yield *Y1* of the preceding solution. Δ*t2* and Δ*t1* are the time intervals from the respective elution to the preceding one and λ_d and λ_p are the half-lives of the daughter and parent nuclides. This formula assumes the constancy of the elution efficacy in between elutions.[21]

Due to the enormous potential in availability and convenient handling for clinical routine, several generator systems based on different parent-daughter nuclide pairs, both for PET and SPECT imaging, have been developed (see table), with the most prominent pair in terms of overall use being the ^{99}Mo/^{99m}Tc-generator.

Daughter nuclide	**Decay Mode**	**$T_{d\ 1/2}$**	**Parent nuclide**	**$T_{p\ 1/2}$**
^{62}Cu	β^+, EC	9.67 min	^{62}Zn	9.19 h
^{68}Ga	β^+, EC	67.63 min	^{68}Ge	270.95 d
^{82}Rb	β^+, EC	1.27 min	^{82}Sr	25.36 d
^{87m}Sr	IT	2.81 h	^{87}Y	79.83 h
^{99m}Tc	IT	6.01 h	^{99}Mo	2.75 d
^{113m}In	IT	1.66 h	^{113}Sn	115.09 d

Figure 6: Commonly used generator nuclides (adapted from [21])

History and development of ^{68}Ge/^{68}Ga-generators

The development of new ^{68}Ga-generators, novel ^{68}Ga-tracers and increasing diagnostic role in PET imaging constituted a revival for the pharmaceutical role of gallium-68. The emission types and half-lives of the ^{68}Ge/^{68}Ga-radionuclide pair are optimal for clinical applications: The relatively long half-life of germanium-68 (270.95 d) allows a long shelf-life of the generator. The half-life of gallium-68 is long enough for radiolabeling and following PET imaging, but short enough in terms of unnecessary radiation exposure for the patient and the staff. Despite these beneficial parameters and availability of early ^{68}Ge/^{68}Ga-generators, gallium-68 only has a high relevance as a PET nuclide since two decades, mainly due to unfavorable qualities of early generators like inert eluted forms of gallium-68.

The first ^{68}Ge/^{68}Ga-generators were based on liquid-liquid extraction (acetylacetone/cyclohexane) and aptly named as a 'positron cow'.[23] Shortly afterwards, a solid-phase ion exchange system with Al_2O_3 as column material was introduced, which was eluted with 0.005 M EDTA.[24] The excellent radiochemical properties allowed the elution of gallium-68 with a yield of 95%. New applications for the so acquired [^{68}Ga]Ga-EDTA were found in brain imaging with limited success depending on the detection method, not only because high doses were required for sufficient image information. Despite the advantageous characteristics of the Al_2O_3 solid-phase ion exchange system, the interest in ^{68}Ga-imaging was haltered. Since [^{68}Ga]Ga-EDTA is thermo-dynamically relatively stable, its complex-chemistry is not feasible for obtaining other ^{68}Ga-complexes. Thus, development of new ^{68}Ga-tracers was severely hindered. Even though procedures to release the gallium-68 cation from its EDTA ligand were attempted, such approaches have not established themselves due to their time-consumption and impracticality.[24] Additionally, huge advances in ^{99m}Tc- and ^{18}F-PET imaging pushed the interest in ^{68}Ga-tracers and their clinical relevance even further aside.

Only when a new ^{68}Ge/^{68}Ga-generator yielding cationic [^{68}Ga]Ga^{3+} was introduced by radiochemists in Obinsk in the early 2000's, gallium-radiochemistry for clinical applications underwent a revival. This type of generators is nowadays based on TiO_2, such as the GalliaPharm® generator by Eckert & Ziegler., which is eluted with hydrochloric acid.[25] The delivered cationic [^{68}Ga]Ga^{3+} was quickly introduced into new ligands using ME(III)-based chemistry with great clinical success, like DOTA. However, novel challenges were also introduced with this method: ^{68}Ge-breakthrough, which increases with the age of the generator, poses concerns in terms of radiation safety and toxicity. Non-radioactive metals such as Zn^{2+} (as a stable decay product of gallium-68) and Fe^{3+} are disturbing factors in the labeling process. These issues were at least in part addressed by post-processing strategies. Directly after elution, a cation- or anion-exchange is introduced in order to remove metal impurities.[26] Alternatively, fractionated elution aids the minimization of these impurities, but even more importantly increases the activity concentration of ^{68}Ga, which is essential for effective radiolabeling.[27] A fractionized elution

protocol with easy handling, which utilizes the activity variation within a single elution volume. By discarding fractions with a low activity (about 20% of the overall activity) and only using the main fraction with the highest activity the labeling contains a high activity concentration without a time investment into further purification.[28]

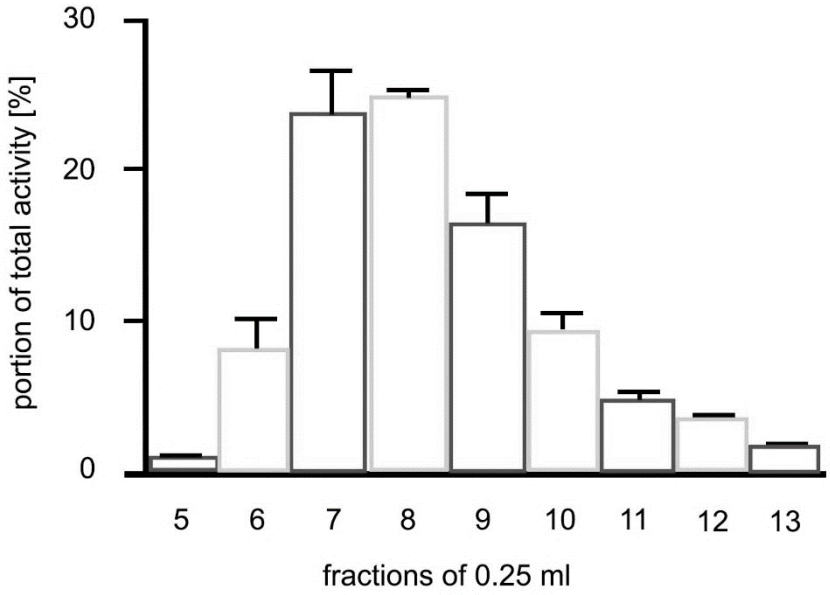

Figure 7: Exemplary profile of a fractionated elution of a gallium-68 generator (adapted from [28])

Microwave assisted synthesis

Microwave assisted synthesis has gathered a lot of interest over the past decades, since almost every name reaction in each discipline of chemistry have been tried with this activation method rather than conventional heating. Many of those reports claim astonishing yields and reduced reaction times, but only mention temperature and power as parameters for the microwave and leave out information (e.g. type of device) that is potentially relevant to reproducibility.[29]

The heating mechanism of microwave devices is based on the principle of dielectric heating rather than on convectional heat transfer, which can be described as a combined process of conduction and advection of molecules in a gaseous or fluid phase. Dielectric heating describes the process of absorption of microwave energy by matter, in which the radiation energy is converted to thermal energy. The electric field component of microwaves causes molecules with mobile dipoles to align according to the field. The dipole moment is therefore necessary for microwave absorption. The response to the electric field, the polarization ***P***, is also dependent on the electric susceptibility χ_e:

$$\boldsymbol{P} = \varepsilon_0 \chi_e \boldsymbol{E}$$

Figure 8: Equation for polarization P[30]

The electric susceptibility χ_e can be derived from the electric permittivity ε of the absorbing medium:

$$\varepsilon = \varepsilon_0 (1 + \chi_e)$$

Figure 9: Equation for the electric permittivity ε[30]

Since this electric field is oscillating with a very high frequency (2.45 GHz is typical for most microwave devices), the dipole alignment of the dipole leads to rotation of the molecule. However, the rotation frequency is lower than the inversion frequency of the electric field, resulting in internal friction and dielectric losses. Field energy is converted to kinetic and thermal energy and thus the medium is heated.[30,31]

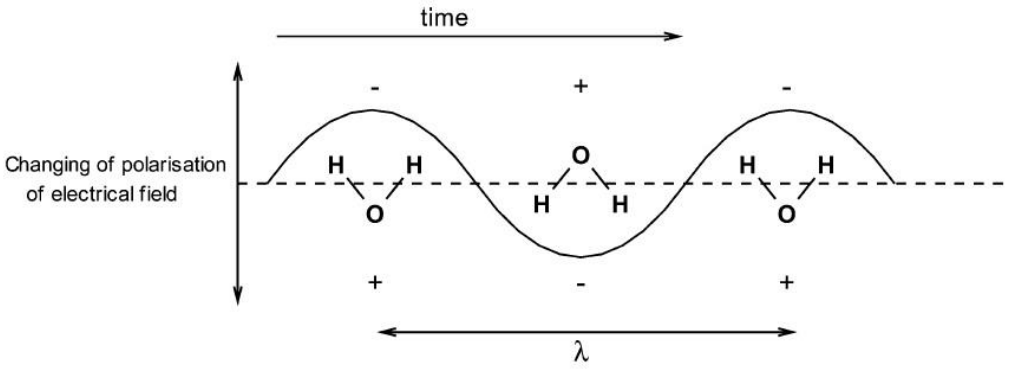

Figure 10: Water dipoles in an alternating electric field [31]

Additionally, due to wave interference by reflection or refraction on surfaces (e.g. boundaries of the reaction vessel) spots with especially high energy absorption lead to local superheating of the solution, similar to boiling delay in unstirred solutions. This overheating effect is often discussed as a contributing factor to the astounding yields of many microwave assisted reactions.[32]

Modern microwave devices are often categorized by the two different possible irradiation methods, monomode and multimode. In monomode devices, the reactor vessel is directly placed in the waveguide. The radiated microwaves, which are reflected in phase, form standing waves. The reactor is placed in the position, where the maximum of a nodal plane of the electric field is calculated in the medium. Consequently, a small reaction volume is preferential (up to 2 mL in this study). In multimode, new patterns of overlaying microwaves can be created by reflection and interference. [33]

Since mercury thermometers are not suitable due to intrinsic microwave absorption, other methods had to be developed. Shielded thermocouples are the cheapest option, but they can act as an antenna to a certain degree und therefore heat up. This can lead to problems in conjunction with some organic solvents. IR-sensors are easily applied in different types of microwave devices by integration outside the reaction vessel. This can lead to considerable margin of error, because the heating occurs within the vessel and the wall is therefore colder, especially for short reactions with steep temperature gradients. Lastly, fiber-optic sensors with gallium arsenide crystals are the most expensive option, but can achieve measurement precision of $\Delta T = 2$ K.[34]

In radiochemistry, overall production time is one of the most important factors for a successful synthesis, especially for short-lived radionuclides. Each time reduction in any necessary step results directly in the increase of the overall activity yield. This makes time-efficient methods like microwave heating very attractive. The production of ^{11}C-radiotracers, mostly starting with [^{11}C]CO_2, profits from a potential time reduction, since the half-life of carbon-11 is only 20 min. In the radiolabeling of [^{11}C]Busulphan, the duration of the cyanodehalogenation leading to [^{11}C]4-hydroxybutyronitrile can be shortened from seven minutes to 30 seconds, as well as the following cyclization step from ten minutes to just one minute compared with regular heating.[35]

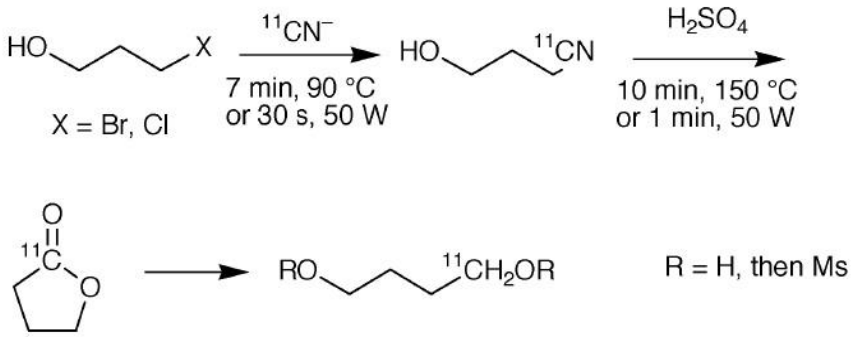

Figure 11: Radiosynthesis of [^{11}C]Busulphan[35]

Even the most produced PET tracer [^{18}F]FDG has been successfully synthesized using a microwave device with time-corrected yields up to 72% with an overall production time of 31 minutes.[36]

Only a few investigations of radiotracer complexation with [^{68}Ga]Ga^{3+} have been reported so far. Velikyan *et al*. labeled DOTA-TOC in a scale of 0.5 - 1 nmol with [^{68}Ga]Ga^{3+} within ten minutes and with an improved specific radioactivity by a factor of 100. This eliminates an additional purification step.[37] Additionally, hexylamine modified and functionalized 17-mer oligonucleotides were conjugated to a DOTA chelator and chelated with gallium-68 using microwave heating with radiochemical yields up to 52% in order to study inhibition of gene expression.[38] Alam *et al.* reported the synthesis of

bis(thiosemicarbazones) and following ^{68}Ga-radiolabeling using microwave irradiation. The radiolabeling was shortened to ten minutes instead of 30 minutes applying conventional heating.[39]

Microfluidic devices in radiosynthesis

Since clinical routine increasingly demands efficient methods for radiotracer synthesis, novel techniques are a worthwhile focus of investigation to make these diagnostic and therapeutic tools easily available to approach a more personalized medicine. Over the last couple of years, the radiosynthesis *via* microfluidic devices gained a lot of attraction for PET-tracer synthesis. Compared to conventional synthesis devices, microfluidic devices distinguish themselves with several advantages: Improved conversion rates, overall fast preparation and reaction time. Most microfluidic devices can be categorized into chip or tubular continuous flow reactors, distinguished by differing design of the channel's geometry. In this study, it is only referring to flow through reactors.

In general, the reactants are loaded into storage loops from separate reservoirs. The reagents are then transferred by individual pumps with adjustable flowrates into a continuous flow reactor, preheated to the reaction temperature. After passage through the reactor, the reaction mixture is collected in a vial. This process can be repeated rapidly depending on the properties of the tubing with product batches in the microliter range.

The miniaturization of the reactor vessel and the down scaling of the tubing diameter in microfluidic devices improves the resilience against pressure, which allows heating with a higher temperature than usually possible, since the boiling point of the used solvents increases with applied pressure.[40] Consequently, radiosyntheses applying microfluidic devices show much higher conversion rates even at low precursor concentration, since conversion rates usually increase with supplied thermal energy to the reactants. Additionally, the conversion rates are also aided by the high surface to volume ratio and the resulting high mass transfer due to the small diameter of the tubing.[41]

The use of very small reaction volumes with microfluidic devices entails several advantages over conventional reactors. This small reaction volume allows the effective handling of highly concentrated solutions. With high radionuclide concentrations, the influence of impurities of the reagents and solvents can be reduced.[42] Furthermore, significant amounts of expensive precursor compound can be saved in the process and low solvent volumes reduces the time during purification.[43] The production of several tracer doses can be conducted in a high frequency and short period of time using a single radionuclide and precursor batch allowing radiotracer production in a dose-on-demand model and decreasing radiation exposure for the operator due to the automatable nature of this technique.[44] This high-throughput of individual radiosyntheses allows the variation of many reaction parameters in a short amount of time and thus is very favorable for the optimization and establishment of novel syntheses.[45]

Microfluidic synthesizers have already been used to good success for the labeling with fluorine-18, surpassing conventional reactor devices in terms of yield and facilitating hitherto infeasible reactions.[46,47] Based on the dose on demand model, several ^{18}F-labeled choline derivatives were

produced by Pascali *et al*. with compelling yields.[48] Furthermore, Selvinova *et al*. successfully conducted the radiofluorination of peptides.[49] Since ^{68}Ga-labeling utilizing the microfluidic approach was not studied intensively at this point, our working group investigated the chelating reaction of [^{68}Ga]Ga-PSMA-11, [^{68}Ga]Ga-DOTA-NOC and [^{68}Ga]Ga-NODAGA-RGDyk, while optimizing the applied reaction parameters with satisfying yields and thus proving this approach suitable for complexation reaction types as well.[50]

Targeting the SST-receptors *via* [^{68}Ga]Ga-DOTA-NOC

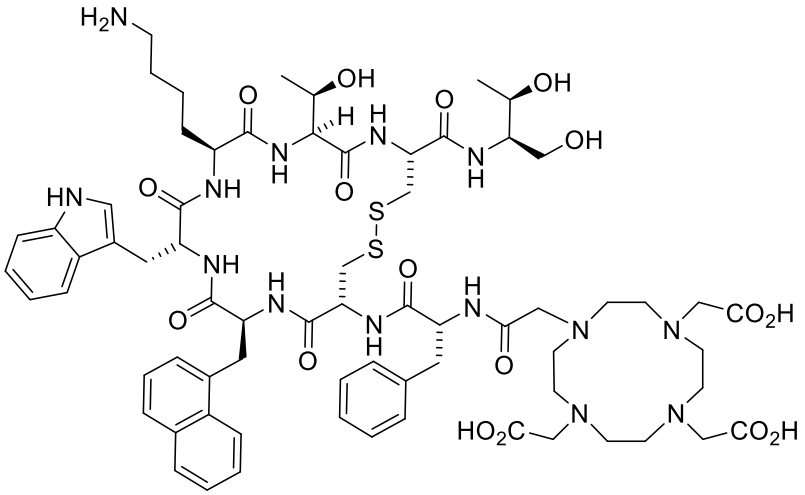

Figure 12: Precursor for [^{68}Ga]Ga-DOTA-NOC

Neuroendocrine tumors (NETs) are a heterogenous group of rare neoplasms with a prevalence of three per 100000, which arise from neuroendocrine cells.[51] They often maintain a secretory function and can lead to hypersecretory syndromes. They may originate from several different organs, including adrenal, thyroid, parathyroid, pituitary gland, pancreas and gut. NETs overexpress somatostatin receptors (SSTR) and thus, are eligible for imaging with radiolabeled somatostatin analogues.[52]

Five different subtypes of SSTR are expressed *in vivo*, while NETs express mainly SSTR2 and SSTR5.[53] Due to the very low lifetime of somatostatin (SST) *in vivo*, stable SST analogues have been developed. SST analogues labeled with long-lived radionuclides like ([^{90}Y]Y-DOTA^{0},Tyr^{3})octreotide and [^{77}Lu]Lu-DOTA-TATE have been introduced as peptide receptor radionuclide therapy for palliative treatment of NETs. ^{68}Ga- or ^{111}In-labeled SSTR agonists as their diagnostic counterpart, such as [^{68}Ga]Ga-DOTA-TOC, [^{68}Ga]Ga-DOTA-NOC ([^{68}Ga]Ga-DOTA,1-Nal$_3$)octreotide and [^{111}In]In- DOTA-octreotide are used as tracers for primary diagnosis, tumor exploration, staging and the evaluation of treatment response to a peptide receptor radionuclide therapy.[54,55]

[^{68}Ga]Ga-DOTA-NOC combines the SSTR agonist D-Phe-cyclo(Cys-1-Nal-D-Trp-Lys-Thr-Cys)-Thr(ol) with the radiometal complexing agent DOTA. [^{68}Ga]Ga-DOTA-NOC shows high affinity to SSTR2, SSTR2 as well as SSTR5, in contrast to its predecessors, with an IC_{50} of 1.9 ± 0.4 nM for SSTR2 and 7.2 ± 1.6 nM for SSTR5, respectively.[56] This broader affinity profile gives [^{68}Ga]Ga-DOTA-NOC a diagnostic advantage over tracers with affinity to a singular SSTR subtype.[57]

Targeting PSMA *via* [^{68}Ga]Ga-PSMA-11

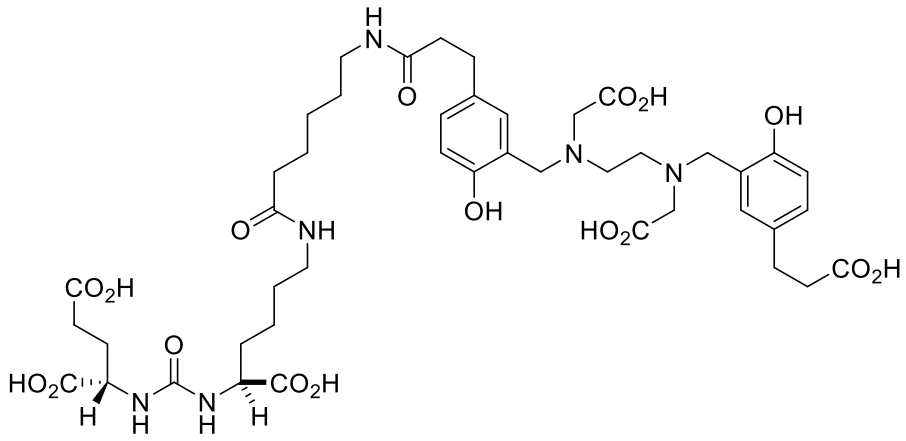

Figure 13: Precursor for [^{68}Ga]Ga-PSMA-11

Prostate cancer is the second most common cancer in men and fourth most common overall with an incidence of 420 in 100000 men over 50.[58] It ranks on top of the most common malignant diseases for males in Austria.[59] Though prostate cancer can be treated effectively, androgen deprivation therapy resistant prostate cancer and metastasized prostate cancer worsen the prognosis drastically. Nuclear medicine offers an alternative therapy approach with targeted radionuclide compounds and unrivalled imaging method for the exploration of metastases. [^{68}Ga]Ga-PSMA is an unprecedented tool in the diagnosis of prostate cancer and its metastases, since it targets PSMA specifically. Through the substitution with a therapeutic nuclide the same target site can be treated with of [^{177}Lu]Lu-PSMA. Combining both, the theranostic radiometal pair gallium-68/ lutetium-177 allows a more personalized approach of medicine, where the success of [^{177}Lu]Lu-PSMA therapy is assessed and controlled by the PET imaging with [^{68}Ga]Ga-PSMA.[9] Despite the decreasing mortality of prostate cancer in countries with higher socioeconomic development, the overall number of deaths caused by prostate cancer increases due to higher incidence rates. Thus, more efficient methods in diagnosis and treatment for

this common malignant disease must be investigated to meet their increasing demand.

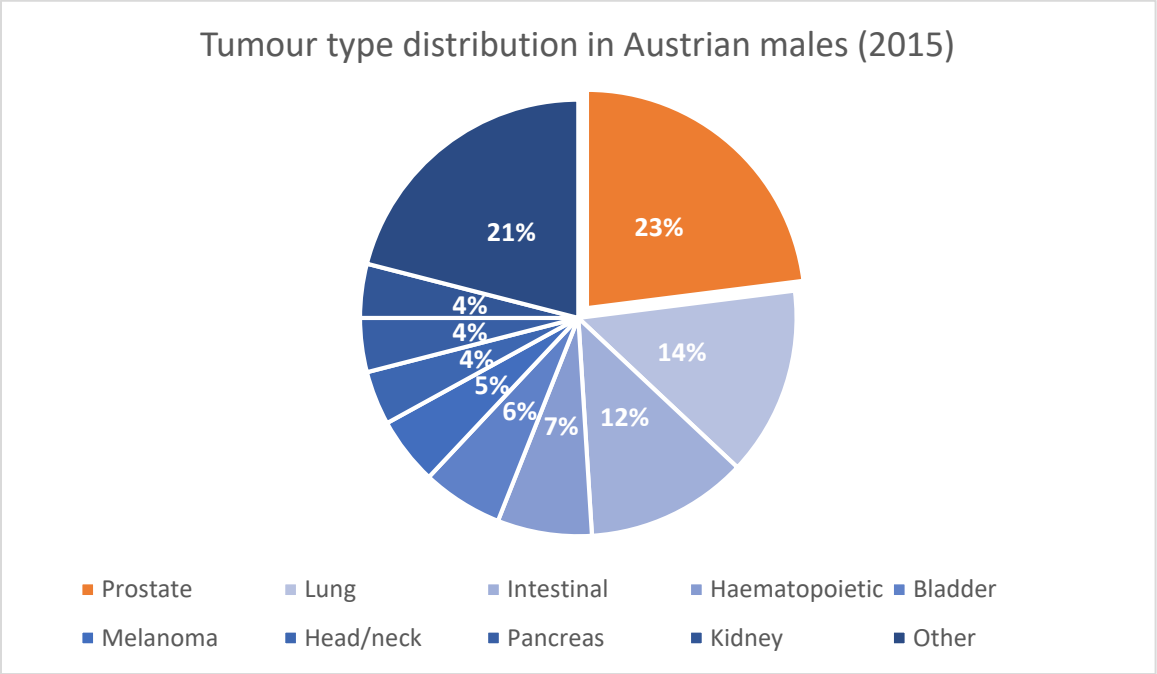

Figure 14: Percentages of malignant diseases in Austrian males (2015)[59]

Prostate-specific membrane antigen (PSMA), also known as glutamate carboxypeptidase II, is a transmembrane enzyme, which facilitates the hydrolysis of N-acetylaspartylglutamate (NAAG) to glutamate and N-acetylaspartate (NAA).[60] It is expressed in healthy prostate tissue as well as in hyperplasia, hypertrophy and cancer of the prostate. PMSA is up-regulated eight to twelve times in prostate cancer compared with physiological prostate levels.[61] Although the role of PSMA for prostate cancer itself is hitherto unknown, the differences in PSMA expression makes it an excellent target for radiolabeled compounds.

[^{68}Ga]Ga-PSMA-11 (synonym: [^{68}Ga]Ga-PSMA-HBED-CC) is a PET-tracer which incorporates the PSMA inhibitor Glu-Urea-Lys and HBED-CC (N,N'-bis-[2-hydroxy-5-(carboxyethyl)benzyl]ethylenediamine-N,N'-diacetic acid) as chelating moiety. This complexing agent shows high affinity to Ga^{3+}, which enables radiolabeling at room temperature.[62] Comparing HBED-CC the radiometal chelator DOTA, showed that the latter did not image prostate cancer tissue at all in a micro PET study.[63] Additionally, the HBED-CC derivative showed 2.6 times higher tumor uptake and 5.7 times lower liver uptake than the DOTA compound. This is likely due to an additional affinity of HBED-CC to a second binding pocket of PSMA.[64] [^{68}Ga]Ga-PSMA-11 showed overall preferable imaging properties with its fast blood clearance and low uptake in organs with low PSMA levels.[64] Although [^{18}F]F-choline PET scans is the standard for metastases exploration in prostate cancer patients, [^{68}Ga]Ga-PSMA-11 outperformed [^{18}F]fluoromethylcholine in terms of image contrast and number of found lesions in a PET/CT study.[65]

Targeting the $\alpha_v\beta_3$ receptor *via* [^{68}Ga]Ga-NODAGA-RGD

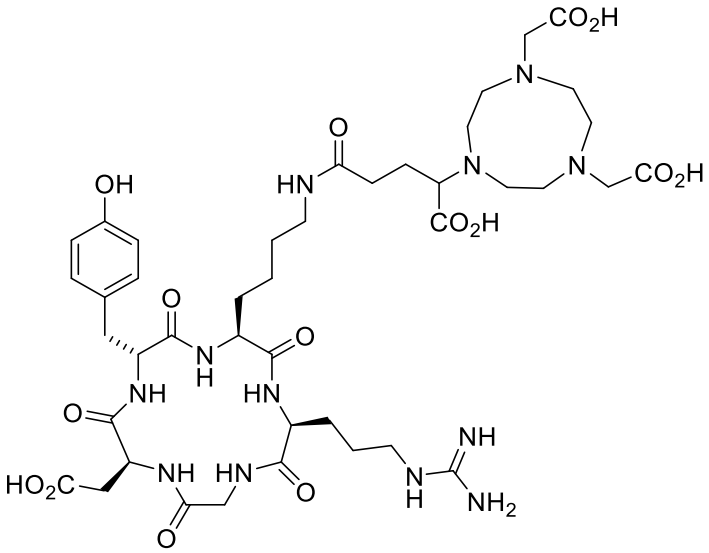

Figure 15: Precursor for [^{68}Ga]Ga-NODAGA-RGDyk

Angiogenesis is the forming of new blood vessels from existing ones, and an important physiological process, which is involved in the pathogenesis of several diseases such as atherosclerosis and rheumatoid arthritis among others.[66,67] Angiogenesis is especially necessary for the progression of malignancies, when a growing tumor reaches a certain size threshold (1 – 2 mm^3) and oxygen and nutrients cannot be supplied by diffusion alone. This process is stimulated by several proteins e.g. growth factors (FGF, VEGF) and integrins.[68]

Integrins are transmembrane glycoprotein receptors consisting of an α and β subunit. They facilitate cell-matrix interaction or the interaction between different cells as receptors and modulators of transmembrane protein kinases.[69] The integrin $\alpha_v\beta_3$ is a receptor for vitronectin, fibrinogen and fibronectin.[70] $\alpha_v\beta_3$ is expressed on activated endothelial cells. However, it is also a factor for tumor growth and for the potential for metastatic progression. This correlation with angiogenic processes makes it a viable target for anti-cancer drug development as well as a potential tool for monitoring the progression of malignant diseases.[71]

The binding epitope of various extracellular matrix proteins like fibrinogen consist of the amino acid sequence arginine-glycine-aspartic acid (RGD). This sequence formed the initial lead structure of the cyclic peptide cyclo(-Arg-Gly-Asp-DPhe-Val) which shows high affinity and selectivity for the $\alpha_v\beta_3$ integrin and was used for the development of radiolabeled tracer molecules.[72] [^{18}F]F-Galacto-RGD as a fluorine labeled tracer showed promising pharmacological properties and specific uptake targeting the $\alpha_v\beta_3$ integrin, but proofed to be unsuitable for clinical use due to its troublesome synthesis.[73] Therefore, the radiometal labeling strategy was applied to circumvent this problem and [^{68}Ga]Ga-DOTA-RGDyk was introduced. Although [^{68}Ga]Ga-DOTA-RGDyk showed specific uptake in

murine tumor models, also high background activity was observed due to a high degree of protein-bond activity.[74] Since the ion radius of Ga^{3+} is too small for an optimal fit in the DOTA chelator, more optimized chelating agents like NOTA (1,4,7-triazacyclononane-N,N',N''-triacetic acid) and the NOTA derivative NODAGA were used in conjugation with a cyclic RGD peptide.[75]

[^{68}Ga]Ga-NODAGA-RGDyk can be synthesized with high yields and radiochemical purity by radiometal chelation, making it suitable for synthesis with automated systems. It selectively targets the $\alpha_v\beta_3$ integrin with sufficient metabolic stability and low background activity due to high protein binding.[76]

II. Aim

The availability of ^{68}Ga-generators and an increasing variety of published ^{68}Ga-tracers increased the need for efficient and fast labeling methods. Therefore, the application of unconventional synthesis methods for the labeling of ^{68}Ga-radiotracers was investigated within this master thesis. One of the methods is microwave heating that achieved astonishing yields and enabled challenging reactions according to literature. This study explores the feasibility of microwave-assisted radiolabeling of [^{68}Ga]Ga-DOTA-NOC, [^{68}Ga]Ga-PSMA-11 and [^{68}Ga]Ga-NODAGA-RGDyk. These compounds are clinically relevant examples for ^{68}Ga-radiotracers with different complexing moieties and addressing different pathophysiological targets. Reaction parameters like precursor concentration, temperature, applied power setting and selected buffer system were evaluated for their influence on radiochemical conversion rates. The potential improvements in the set-up for the microwave-assisted radiolabeling might contribute to clinical applications of this method.

Additionally, [^{68}Ga]Ga-PSMA-11 and [^{68}Ga]Ga-NODAGA-RGDyk were produced applying the technique of microfluidic synthesis. The usage of a microfluidic reactor might offer several advantages like reduced precursor consumption, fast production of individual batches and a streamlined optimization process.

By comparing both methods for those radiotracers, advantages of one technique over the other may be revealed. The results might indicate the appropriate field of application for each modality in a certain clinical setting and with its specific demands.

III. Materials and Methods

Materials

[^{68}Ga]Ga^{3+} was obtained by eluting an Obninsk ^{68}Ge/^{68}Ga-generator (Cyclotron Co., Ltd, Obninsk, Russia) with 0.1 M HCl (Rotem Industries Ltd., Arava, Israel).

The precursor compounds PSMA-11, DOTA-NOC acetate and NODAGA-RGDyk trifluoroacetate were purchased by ABX (GMP-grade, advanced biochemical compounds; Radeberg, Germany).

Ultrapure water for HPLC measurements and precursor solutions for microwave-assisted radiosynthesis was produced by a Milli-Q® Direct Water Purification System (Merck; Darmstadt, Germany). TraceSelect water (Fluka Analytical, Buchs, Switzerland) was used for microfluidic synthesis. Acetonitrile (Sigma-Aldrich, St. Louis, United States), ultrapure water and trifluoro acetic acid (Merck; Darmstadt, Germany) were used for HPLC eluents. Other chemicals for e.g. buffer solutions (HEPES, sodium acetate, ascorbic acid) were of analytical grade and purchased by Sigma-Aldrich. All chemicals were used without further purification.

Microwave-assisted radiosynthesis was performed on a Discover PETwave (CEM Corporation, Matthews, United Stated) using a 2 mL reaction vessel.

Microfluidic-assisted radiosynthesis was conducted an Advion NanoTek microfluidic synthesizer (Ithaca, NY, USA), operated by a control software (Advion, version 1.3.2). It contained a concentrator unit and a liquid flow reaction unit. The reactions were performed in a lead-shielded hot cell (Comecer, Castel Bolognese, Italy).

Thin layer chromatography (TLC) was performed with iTLC-SG glass microfiber chromatography paper impregnated with silica gel (Varian, Lake Forest, Canada) and 0.1 M sodium citrate solution or a 1:1 mixture of 1 M sodium acetate and methanol (adjusted to pH = 4 with HCl) as eluents, respectively. Analysis of radio TLC was evaluated with an instant imager (Canberra-Packard; Schwadorf, Austria).

High performance liquid chromatography (HPLC) was carried out by using an Agilent Technologies 1200 Series HPLC System with a 1100 Series sample collector (Agilent; Santa Clara, United States) and a connected Gabi Star radiodetector (Raytest; Straubenhardt, Germany). Gina Star software was used for peak evaluation. Acetonitrile containing 0.1% TFA and ultrapure water containing 1% TFA were used as mobile phase.

Methods

Elution of the ^{68}Ge/^{68}Ga-generator

Gallium-68 was obtained by elution of a ^{68}Ge/^{68}Ga-generator. The eluate was fractionated, yielding the greatest portion of the activity in a volume of 1.8 mL. In order to assure enough activity for synthesis, the generator was not used for at least 1h or 4 h, so activity was regenerated to yield at least 200 MBq

(for microwave-assisted synthesis) and the maximum activity depending on the generator age for microfluidic synthesis, respectively. Thus, 1.8 mL of [^{68}Ga]Ga^{3+} eluates with activity concentrations of 100 - 250 MBq/mL were used.

General procedure for radiosynthesis using a microwave module

Precursor solutions were prepared from a stock solution of the respective precursor compound in 1 mL of HEPES (1.5 M, pH = 4) or sodium acetate buffer (1 M, adjusted with HCl to pH = 4), respectively. 660 µL of the precursor solution was mixed with 900 µL ^{68}Ga-eluate to obtain a final volume of 1560 µL (pH=4.0 - 4.5). The reaction vessel was immediately sealed with the screw cap manually and heated according to the respective reaction parameters (temperature and power) on 'fixed power'-setting and for 1 min at maximum. After reaching the pre-set temperature, the reaction vessel was cooled by pressured air until reaching temperatures below 40°C and opened samples for quality control were taken. The reactions were performed in a lead shielded area.

Since the empty reaction vessels showed considerable amounts of activity after each reaction, it was washed thrice with 2.5 M HCl and ultrapure water after each synthesis to minimize the residual activity.

General procedure for radiosynthesis using a microfluidic device

Radiolabeling with gallium-68 with the microfluidic device was performed as one-step reaction. The ^{68}Ga-eluate was placed in the concentrator unit connected to the pump numbered 2 (Figure 17), while the precursor solution (in 1.5 M HEPES buffer, pH = 4) in an Eppendorf vial was connected to the pump numbered 1. Equal volumes of both reactants (90 or 360 µL) were loaded in the respective storage loops and then simultaneously transferred through the preheated flow through reactor (25, 100 or 150°C) at 80 µL/min. After completion, the system was swept with TraceSELECT® water. Samples were taken directly from the product solution for quality control. After performing the experiments, a washing program with TraceSELECT® water was run, but not in between individual reactions.

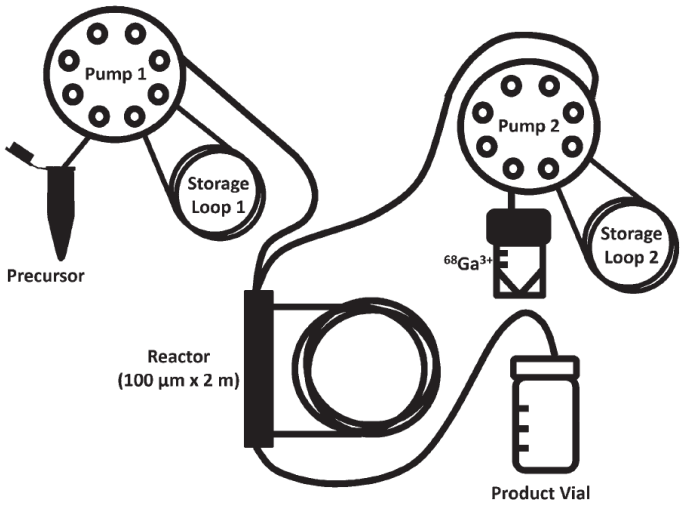

Figure 16: Scheme of the Advion Nanotek LF synthesizer used for ^{68}Ga-radiolabeling[50]

Quality control

Product identity and radiochemical conversion rate (RCR) was confirmed and investigated by radio-TLC (thin layer chromatography) and radio-HPLC (high performance liquid chromatography).

For HPLC analysis an injection volume of 10 µL was chosen using an automatic sample collector, immediately after radiosynthesis. For [^{68}Ga]Ga-PSMA-11 and [^{68}Ga]Ga-DOTA-NOC a HPLC run of 10 min, flow rate of 2 mL/min and a linear gradient of ACN from 5% up to 50% (0.6 - 6.0 min, isocratic flow for 1 min and decreasing gradient down to 5% from 7.0 min to 7.5 min; see figure 18) was used.

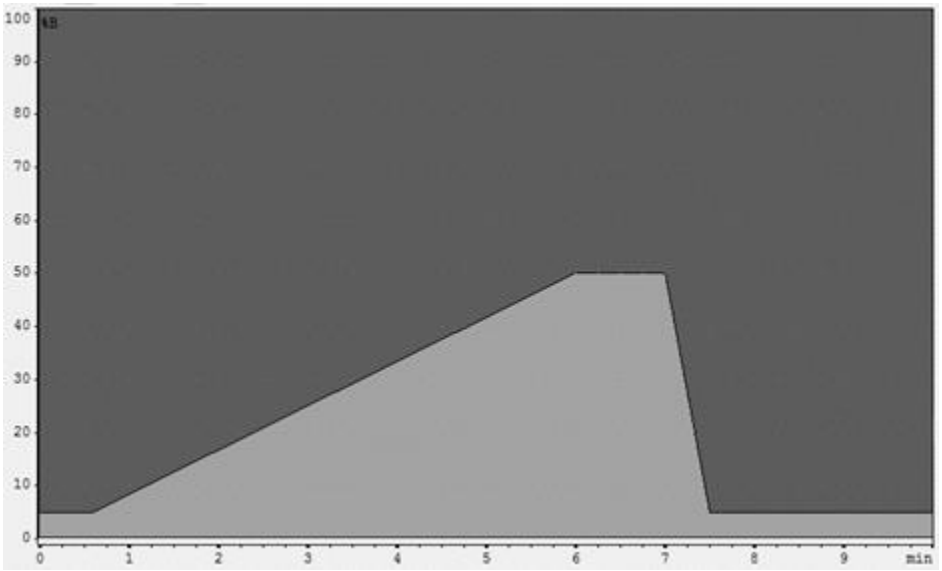

Figure 17: Solvent gradient for the [^{68}Ga]Ga-PSMA-11 and [^{68}Ga]Ga-DOTA-NOC HPLC method: %B is the ACN percentage.

[^{68}Ga]Ga-NODAGA-RGDyk was quantified with a 15 min HPLC run, a flow rate of 2.0 mL/min and an ACN gradient from 3% up to 95% (linear gradient up to 60% from 2.0 min to 8.0 min, up to 95% at 9.0 min and isocratic till 12.0 min, decreasing gradient to 5% at 12.5 min, see figure 19).

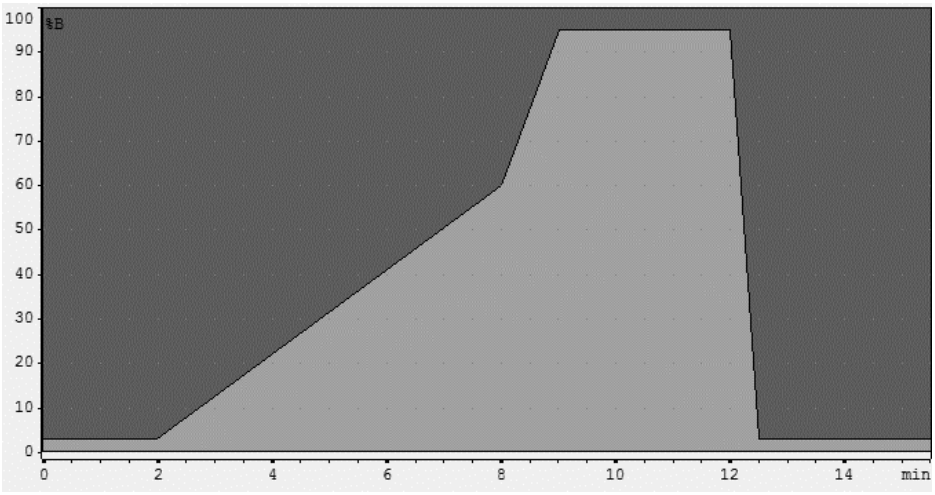

Figure 18: Solvent gradient for the [^{68}Ga]Ga-NODAGA-RGDyk HPLC method: %B is the ACN percentage.

TLC-slices were prepared by cutting the chromatography paper in 2 cm wide pieces and marking the starting line. 3 µL of the product were spotted on the TLC strips immediately after radiosynthesis. The radio-TLC slices were developed with 1 M ammonium acetate/ MeOH 1:1 for [^{68}Ga]Ga-DOTA-NOC and [^{68}Ga]Ga-NODAGA-RGDyk or 0.1 M sodium citrate solution (pH = 5) for [^{68}Ga]Ga-PSMA-11. After drying on a heating plate, the TLC slices were analyzed with an instant imager.

Finally, the radiochemical conversion rate (RCR [%]) was calculated as the product of the purity determined by radio-HPLC and the purity determined by radio-TLC. It is given as mean values ± standard deviation (SD). ANOVA tests (or t-tests for groups of two) were conducted with Graphpad Prism 6 (Graphpad software, La Jolla, U.S.A.). Differences of values were considered as statistically significant with $P \leq 0.05$.

The optimization experiments with the microwave modality were carried out for each ^{68}Ga-labeled tracer by varying one parameter and keeping the other parameters constant. Considered parameters were precursor concentration, temperature, power of the microwave heating and used buffer (Figure 20 - 22). Each experiment with a certain parameter constellation was performed at least thrice.

[^{68}Ga]Ga-DOTA-NOC

Variable	I. Concentration [µg/mL]	II. Concentration [µg/mL]	I. Temperature [°C]	II. Temperature [°C]	Power [W]
Tested Values	0.85 |1.27 | 1.70 2.12 | 2.82	0.85 |1.27 | 1.70 2.12 | 2.82| 4.23	85 | 90 | 95 | 100	85 | 90 | 95 | 100	50 | 100
Conditions	T = 85°C P = 50 W 1.5 M HEPES	T = 90°C P = 50 W 1.5 M HEPES	c = 2.12 µg/mL P = 50 W 1.5 M HEPES	c = 2.82 µg/mL P = 50 W 1.5 M HEPES	c = 2.12 µg/mL T = 95°C 1.5 M HEPES

Figure 19: Overview of all tested reaction parameters for the microwave-assisted synthesis of [^{68}Ga]Ga-DOTA-NOC

[^{68}Ga]Ga-NODAGA-RGDyk

Parameter	Concentration [µg/mL]	Temperature [°C]	Power [W]
Tested Values	0.0577 |0.0865 | 0.115 0.144 | 0.288 | 0.577 1.73 | 2.88 | 5.77	40 | 60 |80 | 100	50 | 100
Conditions	T = 100°C P = 100 W 1.5 M HEPES	c = 0.115 µg/mL P = 100 W 1.5 M HEPES	c = 0.115 µg/mL T = 100°C 1.5 M HEPES

Figure 20: Overview of all tested reaction parameters for the microwave-assisted synthesis of [^{68}Ga]Ga-NODAGA-RGDyk

[^{68}Ga]Ga-PSMA-11

Parameter	Concentration [µg/mL]	Temperature [°C]	Power [W]	Buffer-System
Tested Values	0.0577 | 0.144 | 0.288 0.577	70 | 80 |90 | 100	25 | 50 | 100	HEPES | NaAcO (+/- AA)
Conditions	T = 100°C P = 100 W HEPES	c = 0.144 µg/mL P = 100 W HEPES	c = 0.144 µg/mL T = 100°C HEPES	c = 0.144 µg/mL T = 100°C P = 100 W

Figure 21: Overview of all tested reaction parameters for the microwave-assisted synthesis of [^{68}Ga]Ga-PSMA-11

IV. Results and Discussion

The microwave-assisted synthesis of [^{68}Ga]Ga-DOTA-NOC, [^{68}Ga]Ga-PSMA-11 and [^{68}Ga]Ga-NODAGA-RGDyk was evaluated as examples for peptide tracers with different chelating agents and pathophysiological targets. Precursor concentration, temperature, power setting and influence of applied buffer-system were evaluated as reaction parameters. Distinct radio-HPLC peaks were identified for [^{68}Ga]Ga-DOTA-NOC at 3.5 - 5.0 min, for [^{68}Ga]Ga-PSMA-11 at 4.5 to 6.0 min and for [^{68}Ga]Ga-NODAGA-RGDyk at 4 to 6 min, respectively. Radio-TLC peaks were identified with a R_f= 0.8 - 1.0 for [^{68}Ga]Ga-DOTA-NOC and [^{68}Ga]Ga-NODAGA-RGDyk and R_f < 0.5 for [^{68}Ga]Ga-PSMA-11.

Microwave-assisted radiosynthesis of [^{68}Ga]Ga-DOTA-NOC

Influence of precursor concentration on [^{68}Ga]Ga-DOTA-NOC microwave synthesis

The concentration dependence of [^{68}Ga]Ga-DOTA-NOC radiolabeling *via* microwave was evaluated by two test series with precursor concentrations varying from 0.846 µg/mL to 4.23 µg/mL and other parameters held constant (85°C, 50 W, 1.0 M HEPES-buffer).

The first test series was performed at 85°C and 50 W for the concentrations 0.846 µg/mL, 1.27 µg/mL, 1.70 µg/mL, 2.12 µg/mL and 2.82 µg/mL. As expected, the highest RCR was yielded at the highest tested precursor concentration (93.0 ± 3.9% for 2.82 µg/mL). A trend of the RCR with increasing concentrations with an outlier at 2.12 µg/mL was observed. Lowered precursor concentration resulted in overall lower RCR averages with very high standard deviations (37.2 ± 46.3% for 0.846 µg/mL e.g.). No significant difference in RCR between the tested precursor concentrations could be shown in statistical analysis (Figure 23). However, the highest concentration showed the lowest standard deviation revealing a higher reproducibility.

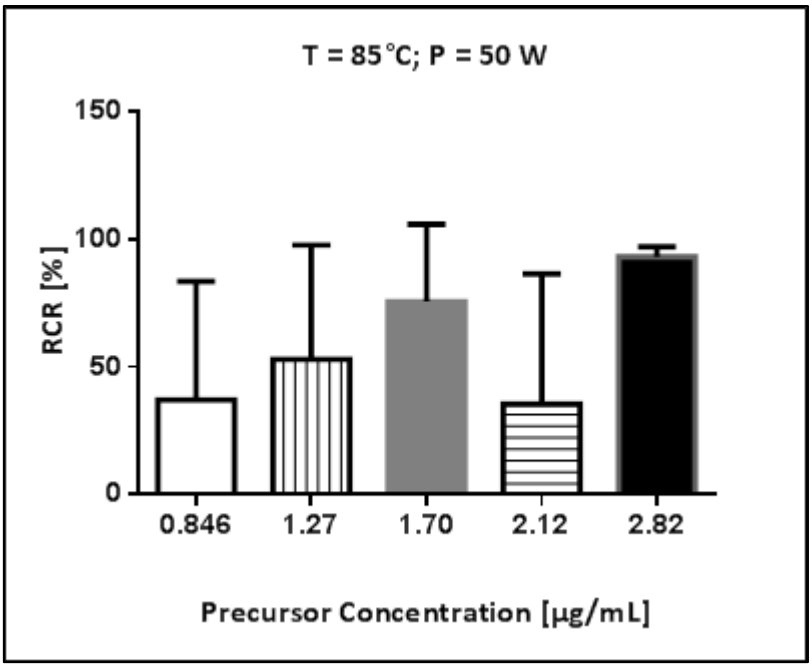

Figure 22: Comparison of RCR in microwave synthesis of [^{68}Ga]Ga-DOTA-NOC at T = 85°C, P = 50 W and varying precursor concentrations

Further experiments at 90°C and with an additional, highest precursor concentration of 4.23 µg/mL was performed and plotted. Although the average RCR is lower for the lower concentration compared to the highest (0.29 ± 0.35 for 0.846 µg/mL and 0.80 ± 0.22 for 4.23 µg/mL, respectively), no linear trend can be observed for these precursor concentrations. The only significant difference in RCR is shown between 2.12 µg/mL and the higher concentrations, as the RCR value for 2.12 µg/mL of 3.6 ± 2.1% results from three failed syntheses attempts, coincidentally (Figure 24). Both test series expressed high values of standard deviation but also occasional near quantitative conversion rates with poor reproducibility. This might imply the infeasibility or at least instability of this method for [^{68}Ga]Ga-DOTA-NOC.

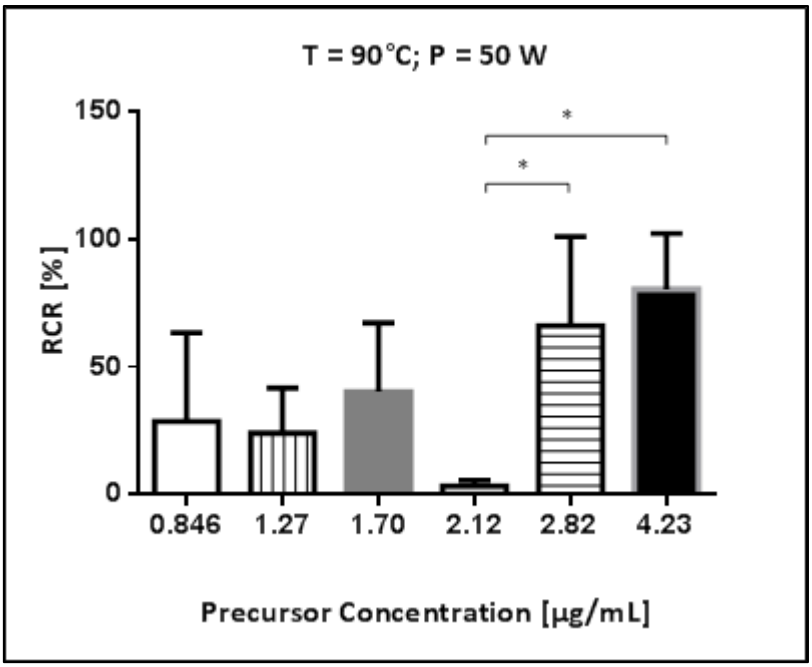

*Figure 23: Comparison of RCR in microwave synthesis of [^{68}Ga]Ga-DOTA-NOC at 90°C, 50 W and varying precursor concentrations ($p < 0.1$ *)*

Influence of temperature on [^{68}Ga]Ga-DOTA-NOC microwave synthesis

The temperatures 85°C, 90°C, 95°C and 100°C were tested at 50 W and in HEPES buffer for the precursor concentrations 2.12 µg/mL and 2.82 µg/mL in two separate test series. Low temperatures were excluded, because the complexation of the DOTA-moiety with [^{68}Ga]Ga^{3+} is known to lead to poor conversion rates at low temperatures[77] and temperatures over the boiling point of the solvent are not applicable for the used microwave device, according to the manufacturer.

In the series with a precursor concentration of 2.12 µg/mL, the highest RCR was achieved at 100°C with a mean of 64.7 ± 53.2%, of which two complexations were near quantitative (95.1% and 95.5%) and one showed relatively low RCR (3.3%). As a result, the SD was for those experiments was high indicating poor reproducibility (Figure 25). Although the mean RCR was lower for the lower temperatures, a trend with an outlier at 85°C but without significant differences between the tested temperatures became apparent.

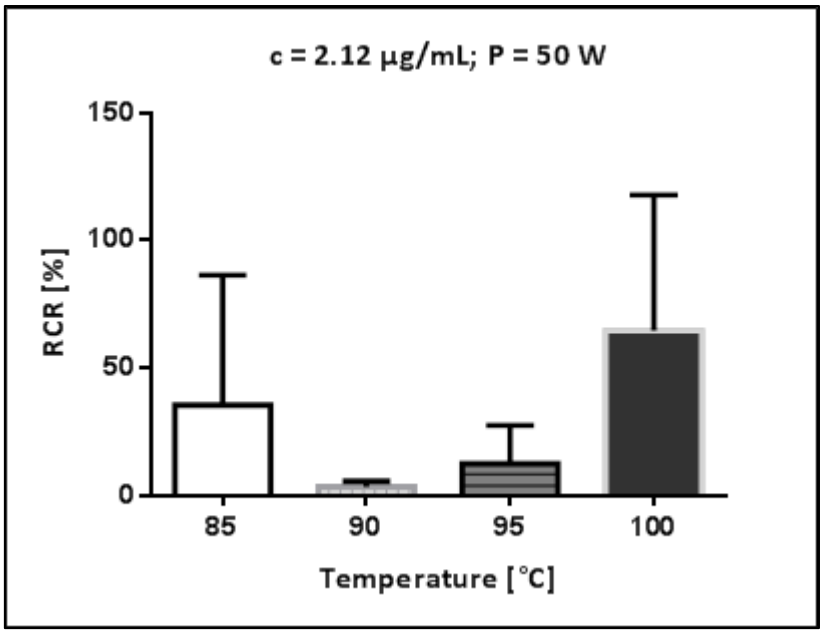

Figure 24: 1st comparison of RCR in microwave synthesis of [^{68}Ga]Ga-DOTA-NOC with 2.12 µg/mL precursor concentration, 50 W and varying temperatures

With a precursor concentration of 2.82 µg/mL, each tested temperature except for 90°C resulted in a mean RCR of 91.3% or higher. No significant differences between the temperature values could be shown here (Figure 26). Compared to the series with a precursor concentration 2.12 µg/mL, remarkably higher RCR values with decreased standard deviations were achieved with 2.82 µg/mL. Those results imply a stronger dependence of RCR and its reproducibility on used precursor concentration rather than temperature in the considered range.

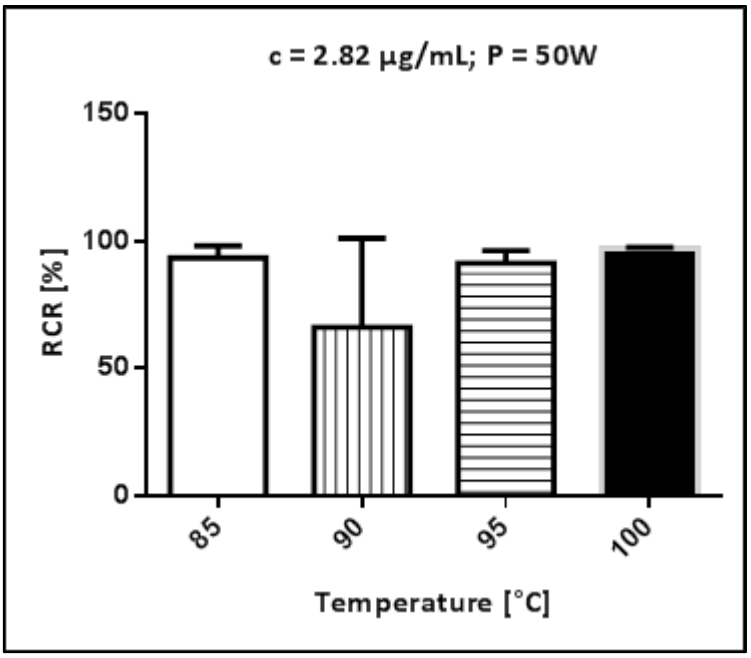

Figure 25: 2nd comparison of RCR in microwave synthesis of [^{68}Ga]Ga-DOTA-NOC with 2.82 µg/mL precursor concentration, 50 W and varying temperatures

Influence of power on [^{68}Ga]Ga-DOTA-NOC microwave synthesis

The used power for microwave heating was tested with a precursor concentration of 2.12 µg/mL at 95°C in HEPES buffer, comparing 50 W to 100 W. Microwave heating of a reaction volume of 1.56 mL took 50 - 55 s using 50 W and 35 - 40 s using 100 W.

No significant difference in RCR could be found using 50 W and 100 W (Figure 27). It is arguable, that a longer reaction time by lowering the power setting might increase RCR. However, almost quantitative conversion was also seen in some reactions in under 1 min.

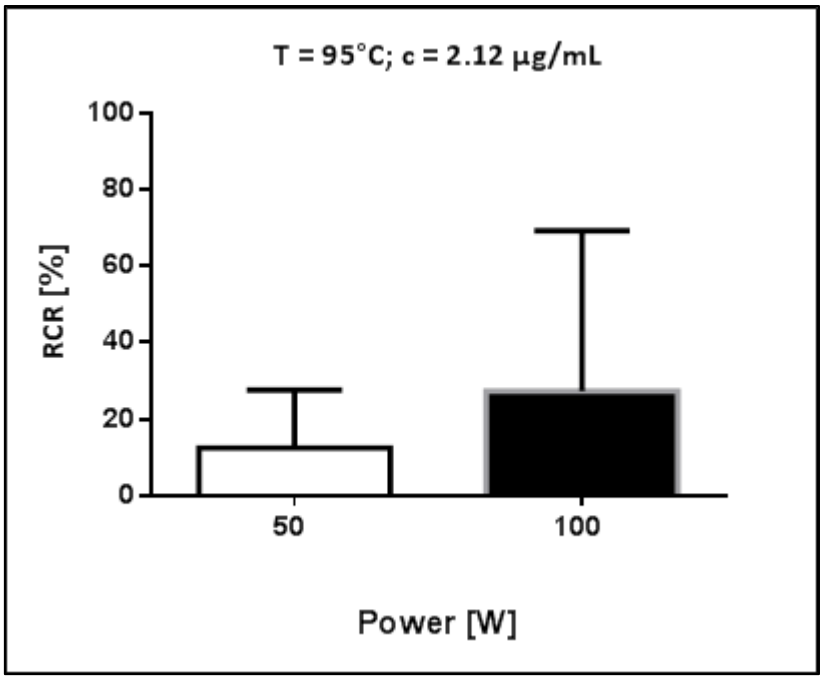

Figure 26: Comparison of RCR in microwave synthesis of [^{68}Ga]Ga-DOTA-NOC with 2.12 µg/mL precursor concentration, 95°C and different power

Evaluation of [^{68}Ga]Ga-DOTA-NOC microwave synthesis

[^{68}Ga]Ga-DOTA-NOC has been successfully radiolabeled utilizing a microwave device with a radiochemical conversion rate of 97.0 ± 0.5% (2.82 µg/mL, 100°C, 50 W) with a reaction time under 1 min. In terms of time efficiency and precursor consumption, this method might rival other established radiolabeling methods of [^{68}Ga]Ga-DOTA-NOC, like single vial kits (50 µg/mL, 10 min)[78] and the TRACERlab FX_{FN} synthesis module (20 µg/mL, 5 min)[79]. Individual reactions with precursor concentration even as low as 0.85 µg/mL showed RCRs up to 95%. However, for most parameter constellations huge deviations in conversion rate were apparent and thus were not reproducible. Thus, the optimum for temperature or precursor concentration was probably not identified. An increase in reaction time might improve the RCR, like shown in a study by Yagi *et al.* There, a RCR of over 95% for [^{68}Ga]Ga-DOTA-TOC was demonstrated using microwave heating with a reaction time of 2 min and a concentration of 3.5 µM.[80] Velikan *et al.* even showed quantitative RCY values for the microwave-assisted labeling of DOTA-comprising precursors in 1 min using a different microwave device than in this study.[37]

Summarizing, radiolabeling *via* microwave is possible for [^{68}Ga]Ga-DOTA-NOC, distinguishing itself with the ability to produce with small precursor amounts and high time efficiency compared to other methods. However, in this study the microwave-assisted set-up seemed instable for [^{68}Ga]Ga-DOTA-NOC radiolabeling. The optimizing process should be pursued with higher precursor

concentrations, an increased reaction time and a microwave device with the capability to heat over the boiling point of the solvent

Microwave-assisted radiosynthesis of [^{68}Ga]Ga-PSMA-11

Influence of precursor concentration on [^{68}Ga]Ga-PSMA-11 microwave synthesis

The evaluation of used precursor amount for microwave assisted synthesis of [^{68}Ga]Ga-PSMA-11 was conducted for precursor concentrations of 0.0423, 0.106, 0.212 and 0.423 µg/mL. All experiments were performed at T = 100°C and P = 100 W.

Increasing the precursor amount showed a linear trend of enhanced RCR's with statistically significant differences between each concentration (Figure 28). Here, the achieved maximum RCR was 91.0 ± 2.1% for 0.423 µg/mL. In this study, higher precursor amounts seem preferable for the microwave-assisted ^{68}Ga-labeling of PSMA-11, but can be viable with amounts as low as 0.423 µg/mL with sufficient conversion rates (Figure 27).

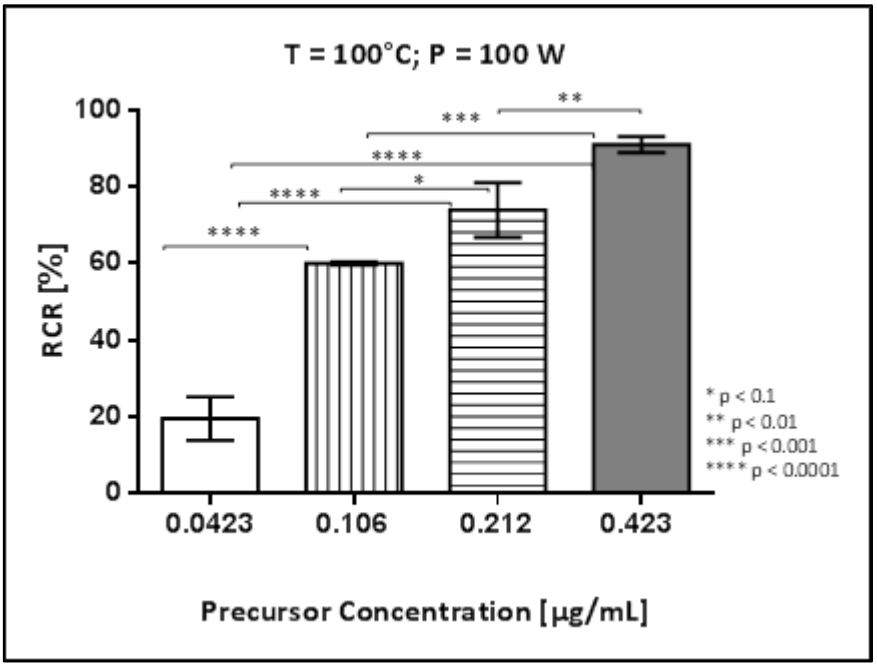

Figure 27: Comparison of RCR in microwave synthesis of [^{68}Ga]Ga-PSMA-11 at 100°C, 100 W and different precursor concentrations

Influence of temperature on [^{68}Ga]Ga-PSMA-11 microwave synthesis

Temperatures of 70, 80, 90 and 100°C were chosen for the evaluation of the temperature parameter in [^{68}Ga]Ga-PSMA-11 microwave synthesis. The reactions were performed at 100 W and a precursor concentration of 0.106 µg/mL. This concentration was selected, since a medium RCR was found in

previous experiments at this concentration and therefore, the observation of a temperature induced benefit might be enhanced. No significant difference in RCR could be found between the tested temperatures. However, the highest reproducibility and conversion rate was found at 100°C (60.0 ± 0.4%), while the highest standard deviation were shown at lower temperatures (46.5 ± 21.6%; 80°C) (Figure 29). Thus, a temperature of 100°C is recommended due to a better reproducibility for this labeling procedure.

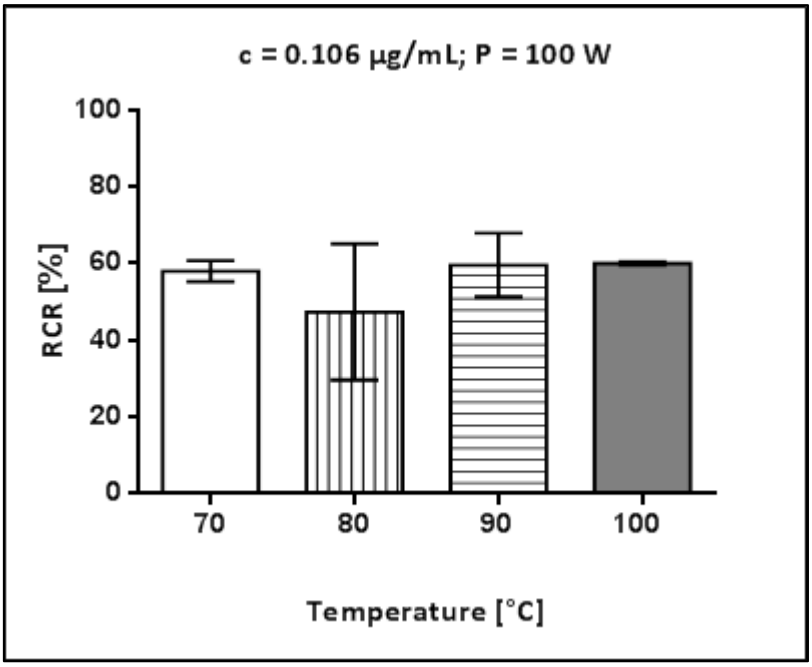

Figure 28: Comparison of RCR in microwave synthesis of [^{68}Ga]Ga-PSMA-11 with 0.106 µg/mL precursor concentration, 100 W and different temperatures

Influence of power on [^{68}Ga]Ga-PSMA-11 microwave synthesis

The power setting of microwave-heating (25, 50 and 100 W) was tested at a precursor concentration of 0.106 µg/mL and a temperature of 100°C. The concentration 0.106 µg/mL was chosen to better elucidate the influence of power. A power of 25 W (49.4 ± 4.9%) showed a significantly reduced RCR compared to 50 and 100 W (64.3 ± 3.6% and 60.0 ± 4.0%, respectively) (Figure 30). Although an increased reaction time at lower power settings (53 – 57 s for 25 W compared to 42 – 48 s for 50 W) might contribute to a higher RCR, but this was not observable here. The better performance might be explained by an increased density of superheating spots in the reaction solution at higher power, which is one of the main explanation models explaining for the generally outstanding capabilities of microwave-assisted synthesis.

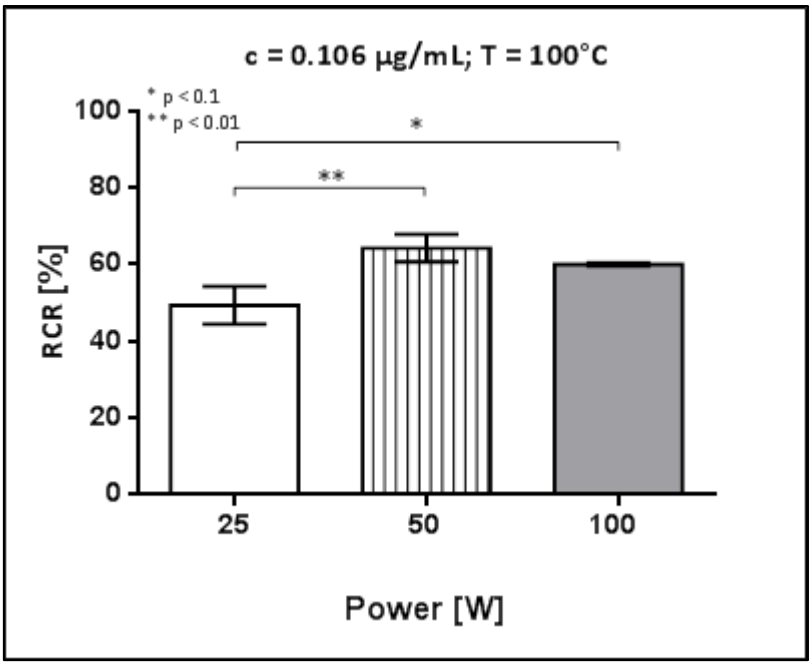

*Figure 29: Comparison of RCR in microwave synthesis of [^{68}Ga]Ga-PSMA-11 with 0.106 µg/mL precursor concentration, 100°C and different powers (p < 0.1 *; p < 0.01 **)*

Evaluation of [^{68}Ga]Ga-PSMA-11 microwave synthesis

[^{68}Ga]Ga-PSMA-11 was successfully synthesized using the microwave device and could represent an option for the acquisition for small, single doses. Increasing the used precursor amount resulted in a linear trend of heightened RCR with near quantitative conversion at 0.423 µg/mL. While different temperatures at a concentration with moderate RCR did not show a benefit for RCR increase, 100°C appeared as the most favorable temperature setting due to its highest reproducibility. The investigation of higher temperatures over the boiling point with an appropriate device might prove beneficial to further extend this advantage. In the evaluation of the power setting, 50 W and 100 W showed a significant difference over 25 W in terms of RCR. Thus, higher power settings should be applied not only for the purpose of shorter reaction times. With reaction times under 1 minute imply potential saving of valuable time compared to other established methods, like kit-based approaches for the synthesis of [^{68}Ga]Ga-PSMA-11 (10 min)[81].

Microwave-assisted radiosynthesis of [^{68}Ga]Ga-NODAGA-RGDyk

Influence of precursor concentration on [^{68}Ga]Ga-NODAGA-RGDyk microwave synthesis

Precursor concentrations ranging from 0.0423 µg/mL to 4.23 µg/mL were tested to evaluate their impact on RCR and to potentially lessen necessary precursor consumption. A temperature of 100°C and an applied power of 100 W were chosen as the highest possible settings to better elucidate the influence of used precursor amount.

A linear progression of enhanced RCR is observable in the concentration range of 0.0635 to 0.423 µg/mL, plateauing into nearly quantitative conversion rates with relatively small standard deviation at precursor concentration 0.423 µg/mL (95.7 ± 1.1 %) and higher (Figure 31). Precursor concentrations of 0.0635 µg/mL or lower showed a conversion below 5 % with relatively high standard deviations.

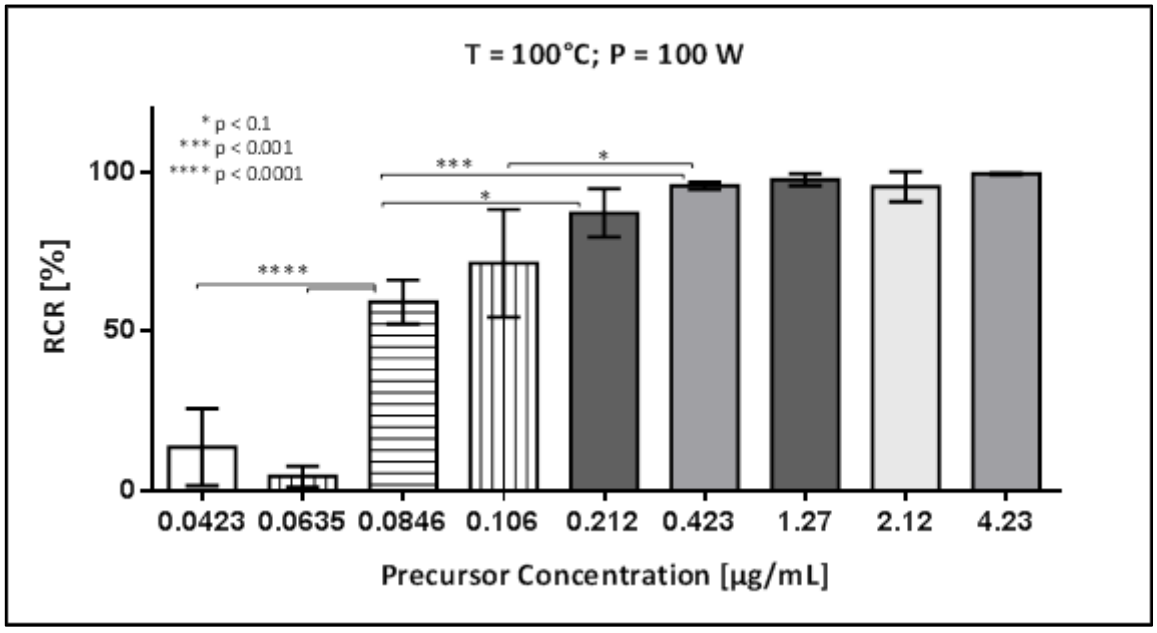

Figure 30: Comparison of RCR in microwave synthesis of [^{68}Ga]Ga-NODAGA-RGDyk at 100°C, 100W and different precursor concentrations

Influence of temperature on [^{68}Ga]Ga-NODAGA-RGDyk microwave synthesis

The influence of temperature on the RCR was assessed at a precursor concentration of 0.0846 µg/mL. to better illustrate the influence of the temperature on conversion rates. 40, 60, 80 and 100°C were considered for this test series, starting at comparably low temperatures, since NODAGA-RGDyk shows complexation with [^{68}Ga]Ga^{3+} even at room temperature[76].

A linear trend of increasing RCR with higher temperatures could be shown for the microwave-assisted ^{68}Ga-labeling of NODAGA-RGDyk (Figure 32). No statistically significant difference between 80°C (56.6 ± 5.0 %) and 100°C (59.2 ± 6.8 %) was shown. However, a slightly higher mean value at 100°C

indicates that a higher temperature could be beneficial by means of RCR. Conversions below 20% occurred even at temperatures as low as 40°C, as to be expected for [^{68}Ga]Ga-NODAGA-RGDyk. Since ^{68}Ga-labeling of NODAGA-RGDyk is possible at room temperature, the low RCR at lower temperatures in this study is most likely due to the short reaction time of < 1 min.

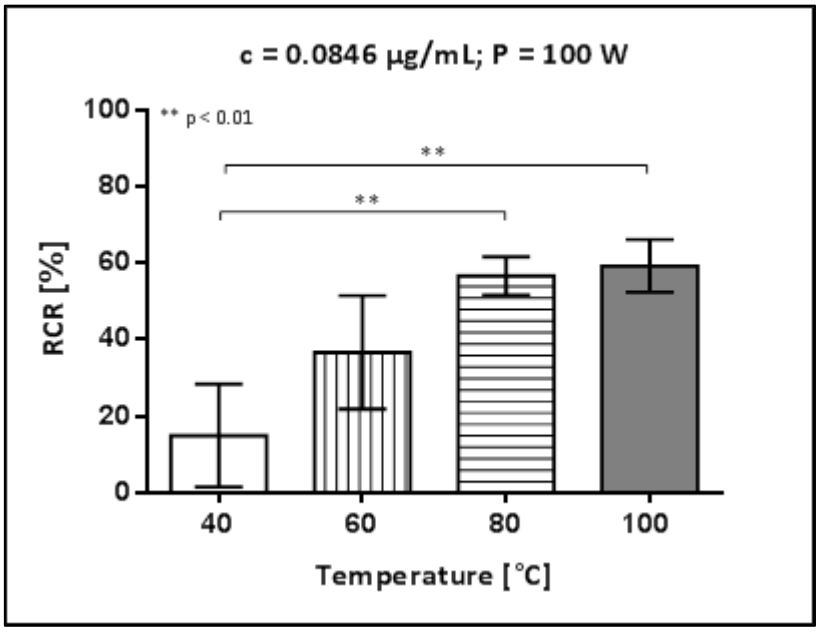

Figure 31: Comparison of RCR in microwave synthesis of [^{68}Ga]Ga-NODAGA-RGDyk with 0.0846 µg/mL precursor concentration, 100 W and different temperatures

Influence of power on [^{68}Ga]Ga-NODAGA-RGDyk microwave synthesis

In addition to the evaluation of the temperature, the applied power setting was investigated at the precursor concentration 0.0846 µg/mL. A temperature of 100°C was applied for those experiments.

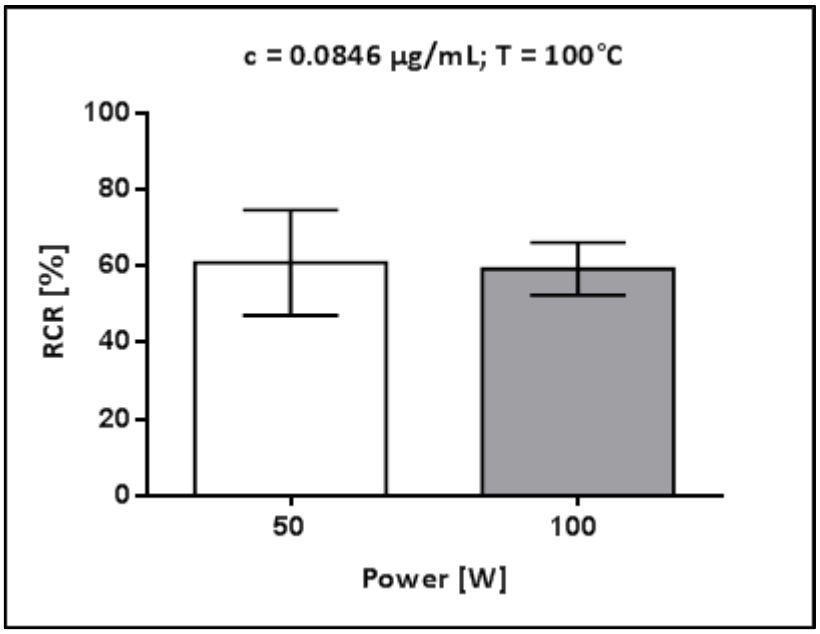

Figure 32: Comparison of RCR in microwave synthesis of [^{68}Ga]Ga-NODAGA-RGDyk with 0.0846 µg/mL precursor concentration, 100°C and a power of 50 W or 100 W.

No statistically significant difference of RCR was shown between the application of 50 W (60.9 ± 13.8 %), and 100 W (59.2 ± 6.8 %) for the microwave-synthesis of [^{68}Ga]Ga-NODAGA-RGDyk (Figure 33). Although the conversion rate was not higher, 100 W might be still be the preferable power setting, since it showed a smaller standard deviation and results in a shorter reaction time.

Evaluation of [^{68}Ga]Ga-NODAGA-RGDyk microwave synthesis

[^{68}Ga]Ga-NODAGA-RGDyk has been successfully synthesized using a microwave-device, as an example for a gallium-tracer with a NODAGA complexing moiety. Similar to [^{68}Ga]Ga-PSMA-11, quantitative RCR's have been approached with precursor concentrations as low as 0.0423 µg/mL with a linear trend for lower concentrations. Even though NODAGA-RGDyk can be labeled with [^{68}Ga]Ga^{3+} at room temperature, a high temperature and power setting of 100°C and 100 W, respectively, should be applied, when using a microwave device with very short reaction times. Compared to the standard protocol by Knetsch *et al.* using conventional heating (0.027 µg/mL, room temperature, 15 min)[76], microwave-assisted synthesis of [^{68}Ga]Ga-NODAGA-RGDyk excels in saving time with reaction times under 1 min. Aa reduction in needed precursor amount could not be achieved with a reaction time under 1 min compared to conventional heating with 15 minutes. However, an outstanding reduction in reaction time using a microwave was shown resulting in excellent RCRs over 95% with precursor concentration as low as 0.423 µg/mL. Consequently, a radioactive decay of 13,3% could be prevented using this method.

Influence of buffer choice on microwave synthesis of ^{68}Ga-radiotracers

The application of different buffer-systems for the microwave-assisted synthesis of [^{68}Ga]Ga-DOTA-NOC, [^{68}Ga]Ga-PSMA-11 and [^{68}Ga]Ga-NODAGA-RGDyk was investigated. 1 M NaAcO (with and without added 10 µM ascorbic acid) and 1.5 M HEPES were used as common labeling buffers. The reactions were performed at 100°C and 100 W. For [^{68}Ga]Ga-PSMA-11, a low and a high precursor concentration (0.106 µg/mL and 0.423 µg/mL) was tested additionally.

Radiolabeling of DOTA-NOC in NaAcO buffer resulted in higher RCR compared to using HEPES, but not for the synthesis with added ascorbic acid (Figure 34). No significant difference was found in statistical analysis between these results due to high standard deviations. NaAcO showed virtually no conversion at a concentration of 0.0846 µg/mL for [^{68}Ga]Ga-NODAGA-RGDyk, while HEPES-buffer yielded a moderate conversion rate of 59.8% (Figure 35). For [^{68}Ga]Ga-PSMA-11, HEPES-buffer also outperformed NaAcO by a significant margin of RCR at a low precursor-concentration of 0.106 µg/mL. The addition of ascorbic acid to the NaAcO-buffer showed no benefit in terms of conversion rates at this concentration. At the higher concentration (0.423 µg/mL), this difference in RCR between NaAcO and HEPES becomes statistically insignificant (Figure 36).

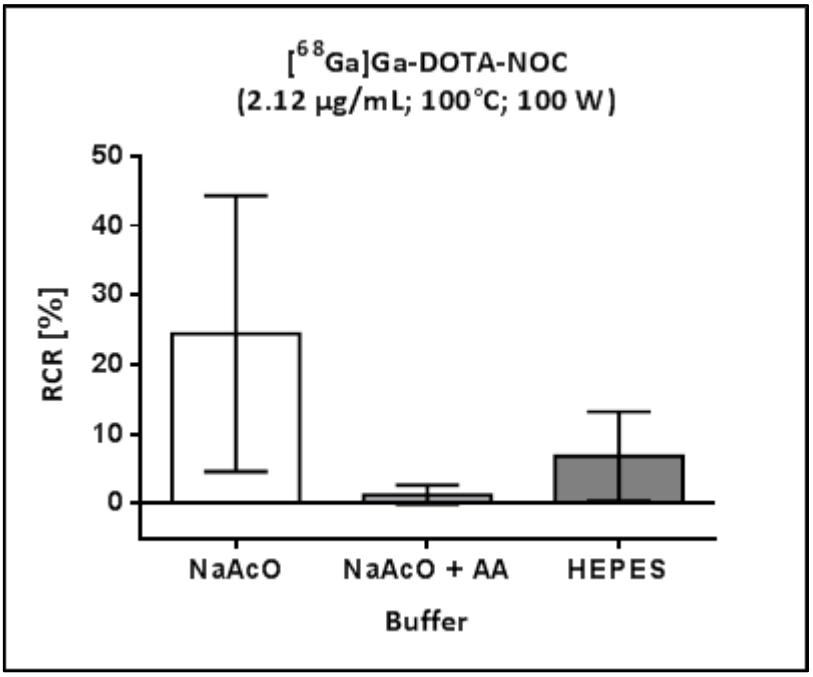

Figure 33: Comparison of RCR using NaAcO or HEPES for the microwave synthesis of [^{68}Ga]Ga-DOTA-NOC

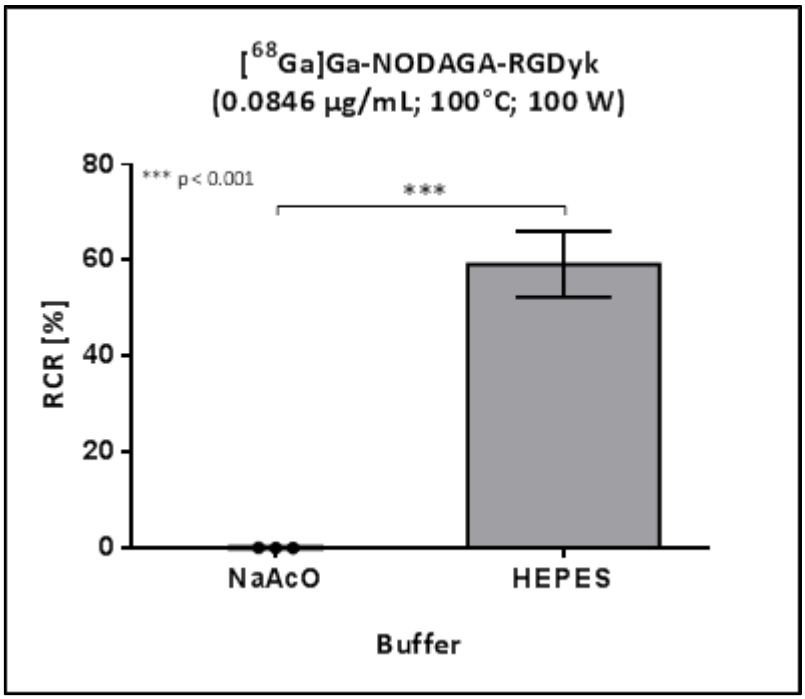

Figure 34: Comparison of RCR using NaAcO or HEPES for the microwave synthesis of [68Ga]Ga-NODAGA-RGDyk

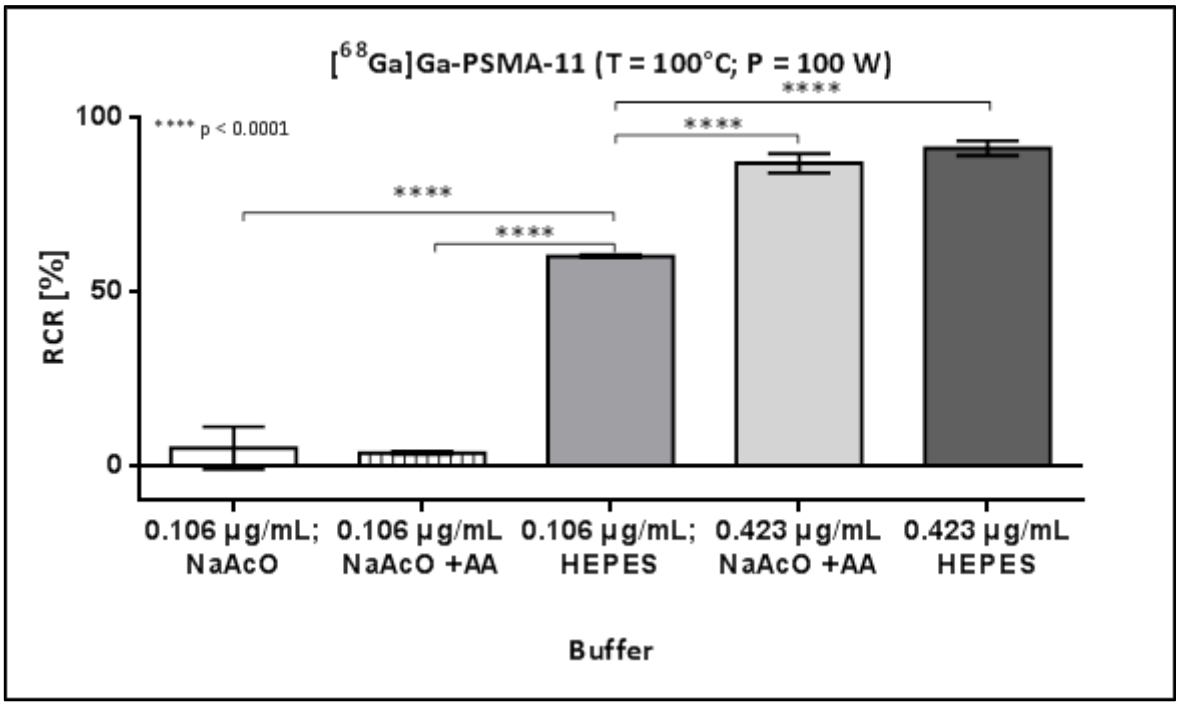

Figure 35: Comparison of RCR using NaAcO or HEPES for the microwave synthesis of [68Ga]Ga-PSMA-11

Comparing RCR, HEPES appears to be the superior buffer over NaAcO for the microwave-assisted synthesis of [68Ga]Ga NODAGA-RGDyk and [68Ga]Ga-PSMA-11. In the case of [68Ga]Ga-PSMA-11, the

difference in RCR was immense at lower precursor concentration, but seems to vanish at higher concentrations. This indicates the application of HEPES-buffer for microwave-assisted ^{68}Ga-labeling, especially at low concentrations and further confirms the known benefit of HEPES over other buffers, as described in the literature.[82] In contrast, the application of NaAcO-buffer resulted in better RCR for [^{68}Ga]Ga-DOTA-NOC in this study. This outcome is contrary against the expectation, since Velykan *et al*. already reported a superior microwave-assisted synthesis of [^{68}Ga]Ga-DOTA-TOC with HEPES-buffer.[83] Both ^{68}Ga-tracers contain the same complexating moiety (DOTA) and thus should yield similar results, theoretically. However, the experiments in this study demonstrated very high standard deviations, which might be explained by utilization of different microwave devices. The buffer-evaluation for [^{68}Ga]Ga-DOTA-NOC should be repeated with an improved set-up, e.g. with a higher precursor concentration.

Microfluidic device-assisted radiosynthesis of ^{68}Ga-labeled tracers

This study investigated the synthesis of clinically relevant [^{68}Ga]Ga-labeled tracers *via* a microfluidic continuous flow system. Precursor concentrations and temperatures were tested for [^{68}Ga]Ga-PSMA-11 and two temperatures for [^{68}Ga]Ga-NODAGA-RGDyk. In order to minimize reaction time, a high flow rate was set (80 µL/min) as long as the experiments were not exceeding the pressure limit of the synthesizer module.

Influence of precursor concentration on microfluidic synthesis of [^{68}Ga]Ga-PSMA-11

A precursor concentration for [^{68}Ga]Ga-PSMA-11 of 5.0 and 7.5 µg/mL was evaluated at a temperature of 100°C and a flowrate of 80 µL/min. Reactions with both concentrations showed satisfactory RCR values over 80% (87.7 ± 14.0% for 5 µg/mL and 83.1 ±8.7% for 7.5 µg/mL). No significant difference was found between both precursor concentrations, but the standard variation was lower for 7.5 µg/mL (Figure 37).

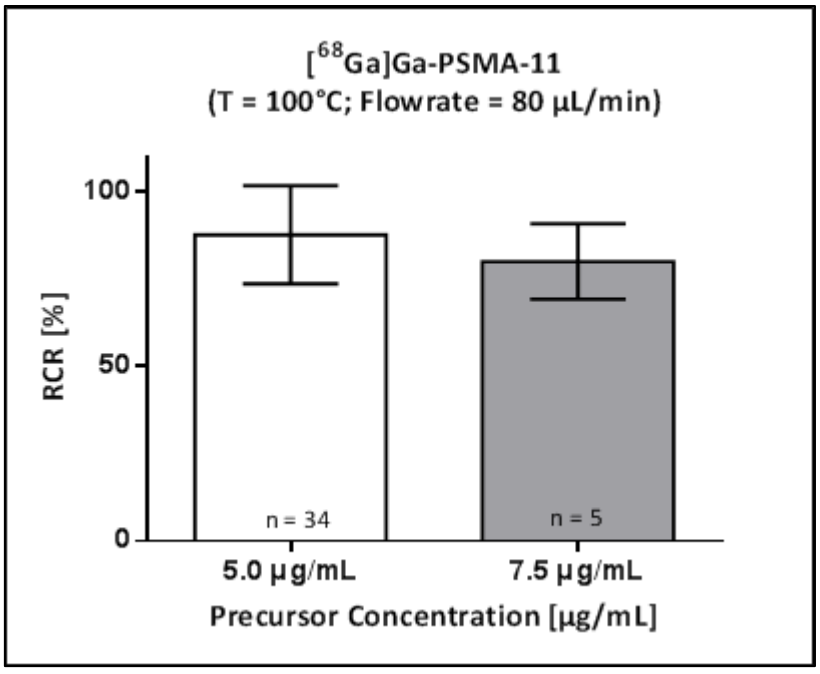

Figure 36: Comparison of RCR in microfluidic synthesis of [^{68}Ga]Ga-PSMA-11 at 100°C, 80 µL/min flowrate and different precursor concentrations

Microfluidic synthesis of [^{68}Ga]Ga-PSMA-11 showed good RCR for both concentrations, which was to be anticipated, since the radiolabeling of PSMA-11 with gallium-68 is well established in general.[1] Even though the mean RCR was higher for 5.0 µg/mL in this experiment series, 7.5 µg/mL might be preferable due to higher reproducibility. Our working group even demonstrated feasible

^{68}Ga-complexation of PSMA-11 with reproducible RCR > 95% in a precursor concentration range of 1 to 5 µg/mL with this method. [50]

Influence of temperature on microfluidic synthesis of [^{68}Ga]Ga-PSMA-11

The reaction temperature for [^{68}Ga]Ga-PSMA-11 was evaluated for 25, 100 and 150°C with a precursor concentration of 5 µg/mL and a flowrate of 80 µL/min. [^{68}Ga]Ga-PSMA-11 was successfully synthesized for each temperature with RCR around 90% (83.1 ± 8.7% for 150°C, 87.7 ± 14.0% for 100°C, and 83.1 ± 8.7% for 150°C). In statistical analysis, no significant difference in RCR could be found between those temperatures, but T = 150°C proved to be the most reproducible (Figure 38).

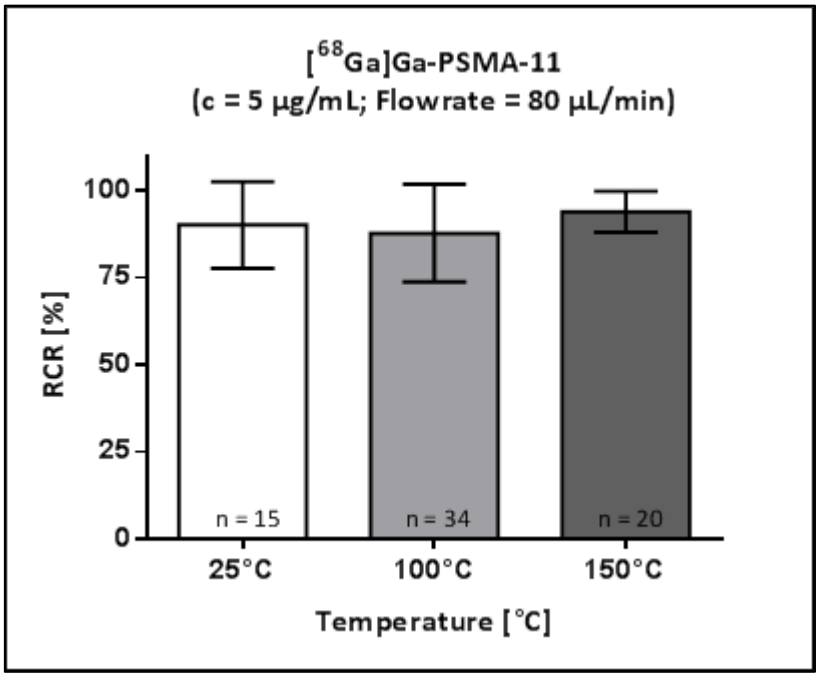

Figure 37: Comparison of RCR in microfluidic synthesis of [^{68}Ga]Ga-PSMA-11 with 5.0 µg/mL precursor concentration, 80 µL/min flowrate and different temperatures

Generally, [^{68}Ga]Ga-PSMA-11 can be produced *via* microfluidic approach with each of the tested temperatures. However, 150°C might be preferable due to highest RCR and best reproducibility. It should be mentioned, that our working group. reported the poorest RCR at 150°C for a precursor concentration of 1.0 µg/mL, potentially caused by precursor decomposition.[50] This was not observed here with 5.0 µg/mL.

Influence of temperature on microfluidic synthesis of [^{68}Ga]Ga-NODAGA-RGDyk

The microfluidic synthesis of [^{68}Ga]Ga-NODAGA-RGDyk was evaluated for T = 25°C and T = 100°C with a precursor concentration of 20 µg/mL and a flowrate of 80 µL/min. Both temperatures resulted in

RCR over 95% (96.8 ± 5.0% for 25°C, and 97.0 ± 1.6% for 100°C) with a very low standard deviation for T = 100°C (Figure 39).

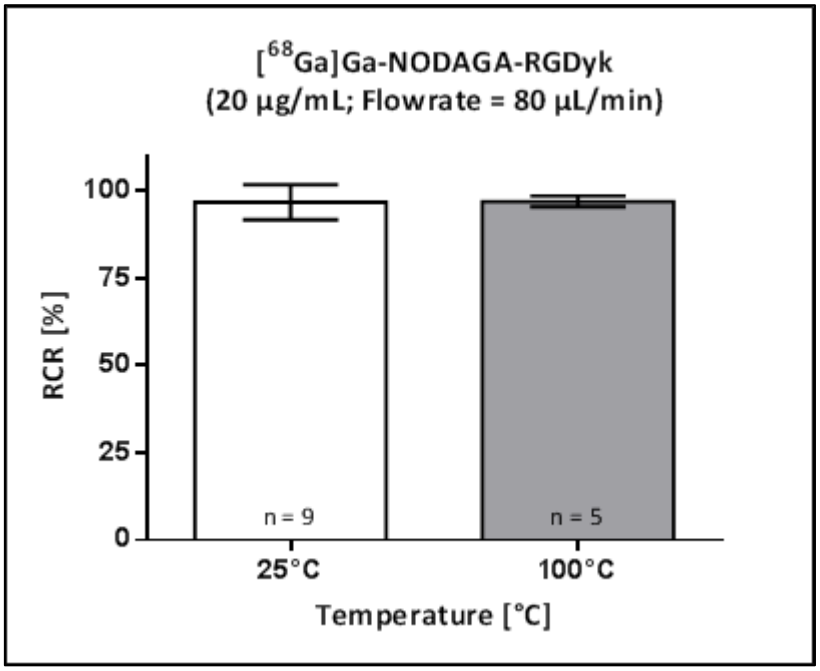

Figure 38: Comparison of RCR in microfluidic synthesis of [^{68}Ga]Ga-NODAGA-RGDyk with 20 µg/mL precursor concentration, 80 µL/min flowrate and different temperatures

At a comparably high precursor concentration of 20 µg/mL, [^{68}Ga]Ga-NODAGA-RGDyk was synthesized with excellent conversion rates for both temperatures. However, a high precursor concentration might be necessary, since microfluidic synthesis of [^{68}Ga]Ga-NODAGA-RGDyk was not feasible with precursor concentrations under 15 µg/mL according to our working group.[50] Even though the RCR showed no significant difference for 25°C and 100°C, high temperatures (e.g. 100°C) might be preferable for their slightly better reproducibility.

Comparison between Microwave- and Microfluidic-assisted ^{68}Ga-labeling

Both modalities allowed the synthesis of each tested ^{68}Ga-radiotracers with very satisfying radiochemical conversion rates over 90% and almost quantitative conversions in the case of a few reactions. In order to compare both methods to some extent, RCR values of reactions conducted at 100°C are displayed (Figure 40).

[^{68}Ga]Ga-Radiotracer	**Microwave-assisted Synthesis**		**Microfluidic Synthesis**	
T = 100°C	Concentration [µg/mL]	RCR ± SD [%]	Concentration [µg/mL]	RCR ± SD [%]
[^{68}Ga]Ga-DOTA-NOC	2.82	97.0 ± 0.4		
[^{68}Ga]Ga-PSMA-11	0.42	91.0 ± 2.1	5.0	87.7 ± 14.0
[^{68}Ga]Ga-NODAGA-RGDyk	4.23	99.3 ± 0.2	20.0	97.0 ± 1.6

Figure 39: Comparison of RCR of [^{68}Ga]Ga-DOTA-NOC, [^{68}Ga]Ga-PSMA-11 and [^{68}Ga]Ga-NODAGA-RGDyk via microwave assisted and microfluidic ^{68}Ga-labeling at 100°C

Microwave-assisted and microfluidic synthesis both achieved very high RCR values for each of their tested ^{68}Ga-tracers. However, microwave-assisted synthesis expressed a low reproducibility for [^{68}Ga]Ga-DOTA-NOC. This was also the case for microfluidic production, when including test data from our working group. In the case of both methods, [^{68}Ga]Ga-PSMA-11 was synthesized with mean RCR around 90%, but showed a higher reproducibility applying a microwave technique. For [^{68}Ga]Ga-PSMA-11, our working group reported a RCR of 93.3 ± 7.5 for a precursor concentration of 0.5 µg/mL, showing similar RCR results for ^{68}Ga-labeling of PSMA-11 with both methods at comparable precursor concentrations. [^{68}Ga]Ga-NODAGA-RGDyk showed excellent RCR values, often approaching quantitative conversion, with both synthesis devices. Here, a precursor concentration of 20 µg/mL was used for the microfluidic synthesis, but which can be as low as 7.5 µg/mL, making both techniques almost equal for this case. Overall, Microwave-assisted synthesis seemed superior to the microfluidic approach in terms of necessary precursor amount und reaction time in this study.

V. Conclusion and Outlook

The aim of the present thesis was to improve radiotracer synthesis by investigating the feasibility of novel synthesis modalities for the time and substance efficient labeling of clinically relevant ^{68}Ga-radiotracers. [^{68}Ga]Ga-PSMA-11, [^{68}Ga]Ga-DOTA-NOC, and [^{68}Ga]Ga-NODAGA-RGDyk were chosen as representatives with different chelating agents and clinical targets. All radiotracers were successfully labeled by microwave-assisted synthesis, a technique commonly applied in almost each field of chemistry and often with astounding success. Adjustable parameters like precursor concentration, temperature and applied power were studied to potentially improve this method. Additionally, [^{68}Ga]Ga-PSMA-11 and [^{68}Ga]Ga-NODAGA-RGDyk were synthesized by utilization of a continuous-flow microfluidic device, as an alternative modality with other unique properties.

Radiolabeling with a microwave device distinguishes itself with very fast reaction times under one minute and low effort for set-up, which gives reason to pursue investigations on this technique for clinical application. With interchangeable reaction-vessels, the reaction volume is adjustable, making it a viable method for the development a KIT-based approach.

In contrast, reactions with a microfluidic device require comparably higher set-up time, mainly due to the loading process of reactant solutions, which is dependent on the length of the used tubing and loops. However, the microfluidic approach can produce consecutive batches of radiotracer on a dose-on-demand principle. For this reason, the screening and optimization process of reaction parameters is highly efficient. Even though this technique is restricted in the case of higher reaction volumes, it excels, when small volumes are required. With the potential future prospect of highly concentrated ^{68}Ga-solutions through cyclotron production, reaction volumes in the microliter- rather than the milliliter-range might be required, granting it a very suitable application. In the case of the specific devices used for this study, microfluidic synthesis alone allowed the heating over boiling point, which can be essential for certain reaction types.

In summary, both synthesis methods investigated in this study were successful in producing the selected ^{68}Ga-radiotracers with good radiochemical conversion rates. Microwave-assisted synthesis was feasible with precursor concentration in the low micromolar range for each radiotracer with RCR over 90% with reaction times under one minute. The microfluidic approach also reached high RCR-values, but was only tested with higher precursor concentration. Additional data generated by our working group showed that, higher concentrations were necessary for sufficient conversion rates. Microfluidic synthesis was also associated with higher time investment in preparation as well as actual reaction time. Nevertheless, a direct comparison of both techniques seems difficult, since both involve certain advantages, unique to the respective method. Microfluidic and Microfluidic synthesis both

could find specialized areas of application, depending on the parameters of clinical demand and specifics of the radiolabeling.

Both methods show much potential and unique properties for improvement in radiotracer production in clinical routine. Hence, the investigation of labeling of other tracers with different radionuclides is likely very worthwhile.

VI. Abbreviations

ACN	Acetonitrile
CT	Computed tomography
DOTA-NOC	L-Cysteinamide, N-[[4,7,10-tris(carboxymethyl)-1,4,7,10-tetraazacyclododec-1-yl]acetyl]-D-phenylalanyl-L-cysteinyl-3-(1-naphthalenyl)- L-alanyl-D-tryptophyl-L-lysyl-L-threonyl-N-[(1R,2R)-2-hydroxy-1-(hydroxymethyl)propyl]-, cyclic (2→7)-disulfide
DOTA-TATE	DOTA-D-Phe-Cys-Tyr-D-Trp-Lys-Thr-Cys-Thr-OH, cyclic disulfide
DOTA-TOC	L-Cysteinamide, N-[[4,7,10-tris(carboxymethyl)-1,4,7,10-tetraazacyclododec-1-yl]acetyl]-D-phenylalanyl-L-cysteinyl-Ltyrosyl-D-tryptophyl-L-lysyl-L-threonyl-N-[(1R,2R)-2-hydroxy-1-(hydroxymethyl)propyl]-, cyclic(2→7)-disulfide
EDTA	Ethylenediaminetetraacetic acid
FDG	Fludeoxyglucose
HCl	Hydrochloric acid
HEPES	4-(2-hydroxyethyl)-1-piperazineethanesulfonic acid
HPLC	High performance liquid chromatography
MeOH	Methanol
MRI	Magnetic resonance imaging
NaOAc	Sodium acetate
NET	Neuroendocrine tumor
NODAGA-RGDyk	Cyclo[L-arginylglycyl-L-α-aspartyl-D-tyrosyl-N6-([[4,7-bis(carboxymethyl)-1,4,7-triazonan-1-yl]acetyl])-L-lysyl]
PET	Positron emission tomography
PSMA	Prostate specific membrane antigen
PSMA-11	Glu-NH-CO-NH-Lys(Ahx)-HBED-CC
RCR	Radiochemical conversion rate
RCY	Radiochemical yield
SD	Standard deviation
SPECT	Single photon emission computed tomography
SST	Somatostatin
SSTR	Somatostatin rezeptor
TFA	Trifluoroacetic acid
TLC	Thin layer chromatography

VII. Figure Caption

Figure 1: Transverse (a) CT, (b) PET, and (c) PET/CT fused images of a thorax with non-small cell lung carcinoma ([18F]FDG.)[6] 2
Figure 2: Structural elements of a PET radiotracer (adapted from [7]) 3
Figure 3: Commonly used radionuclides in nuclear medicine (adapted from [10]) 5
Figure 4: Bateman equation for the determination of the daughter activity Ad(t)[21] 6
Figure 5: Equation for a starting activity after incomplete elution in a generator system[21] 7
Figure 6: Commonly used generator nuclides (adapted from [21]) 7
Figure 7: Exemplary profile of a fractionated elution of a gallium-68 generator (adapted from [28]) 9
Figure 8: Equation for polarization P[30] 10
Figure 9: Equation for the electric permittivity ε[30] 10
Figure 10: Water dipoles in an alternating electric field [31] 10
Figure 11: Radiosynthesis of [11C]Busulphan[35] 11
Figure 12: Precursor for [68Ga]Ga-DOTA-NOC 15
Figure 13: Precursor for [68Ga]Ga-PSMA-11 16
Figure 14: Percentages of malignant diseases in Austrian males (2015)[59] 17
Figure 15: Precursor for [68Ga]Ga-NODAGA-RGDyk 18
Figure 16: Scheme of the Advion Nanotek LF synthesizer used for 68Ga-radiolabeling[50] 22
Figure 17: Solvent gradient for the [68Ga]Ga-PSMA-11 and [68Ga]Ga-DOTA-NOC HPLC method: %B is the ACN percentage. 23
Figure 18: Solvent gradient for the [68Ga]Ga-NODAGA-RGDyk HPLC method: %B is the ACN percentage. 24
Figure 19: Overview of all tested reaction parameters for the microwave-assisted synthesis of [68Ga]Ga-DOTA-NOC 25
Figure 20: Overview of all tested reaction parameters for the microwave-assisted synthesis of [68Ga]Ga-NODAGA-RGDyk 25
Figure 21: Overview of all tested reaction parameters for the microwave-assisted synthesis of [68Ga]Ga-PSMA-11 25
Figure 22: Comparison of RCR in microwave synthesis of [68Ga]Ga-DOTA-NOC at T = 85°C, P = 50 W and varying precursor concentrations 27
Figure 23: Comparison of RCR in microwave synthesis of [68Ga]Ga-DOTA-NOC at 90°C, 50 W and varying precursor concentrations ($p < 0.1$ *) 28

Figure 24: 1st comparison of RCR in microwave synthesis of [^{68}Ga]Ga-DOTA-NOC with 2.12 µg/mL precursor concentration, 50 W and varying temperatures 29
Figure 25: 2nd comparison of RCR in microwave synthesis of [^{68}Ga]Ga-DOTA-NOC with 2.82 µg/mL precursor concentration, 50 W and varying temperatures 30
Figure 26: Comparison of RCR in microwave synthesis of [^{68}Ga]Ga-DOTA-NOC with 2.12 µg/mL precursor concentration, 95°C and different power 31
Figure 27: Comparison of RCR in microwave synthesis of [^{68}Ga]Ga-PSMA-11 at 100°C, 100 W and different precursor concentrations 32
Figure 28: Comparison of RCR in microwave synthesis of [^{68}Ga]Ga-PSMA-11 with 0.106 µg/mL precursor concentration, 100 W and different temperatures 33
Figure 29: Comparison of RCR in microwave synthesis of [^{68}Ga]Ga-PSMA-11 with 0.106 µg/mL precursor concentration, 100°C and different powers ($p < 0.1$ *; $p < 0.01$ **) 34
Figure 30: Comparison of RCR in microwave synthesis of [^{68}Ga]Ga-NODAGA-RGDyk at 100°C, 100W and different precursor concentrations 35
Figure 31: Comparison of RCR in microwave synthesis of [^{68}Ga]Ga-NODAGA-RGDyk with 0.0846 µg/mL precursor concentration, 100 W and different temperatures 36
Figure 32: Comparison of RCR in microwave synthesis of [^{68}Ga]Ga-NODAGA-RGDyk with 0.0846 µg/mL precursor concentration, 100°C and a power of 50 W or 100 W 37
Figure 33: Comparison of RCR using NaAcO or HEPES for the microwave synthesis of [^{68}Ga]Ga-DOTA-NOC 38
Figure 34: Comparison of RCR using NaAcO or HEPES for the microwave synthesis of [^{68}Ga]Ga-NODAGA-RGDyk 39
Figure 35: Comparison of RCR using NaAcO or HEPES for the microwave synthesis of [^{68}Ga]Ga-PSMA-11 39
Figure 36: Comparison of RCR in microfluidic synthesis of [^{68}Ga]Ga-PSMA-11 at 100°C, 80 µL/min flowrate and different precursor concentrations 41
Figure 37: Comparison of RCR in microfluidic synthesis of [^{68}Ga]Ga-PSMA-11 with 5.0 µg/mL precursor concentration, 80 µL/min flowrate and different temperatures 42
Figure 38: Comparison of RCR in microfluidic synthesis of [^{68}Ga]Ga-NODAGA-RGDyk with 20 µg/mL precursor concentration, 80 µL/min flowrate and different temperatures 43
Figure 39: Comparison of RCR of [^{68}Ga]Ga-DOTA-NOC, [^{68}Ga]Ga-PSMA-11 and [^{68}Ga]Ga-NODAGA-RGDyk *via* microwave assisted and microfluidic ^{68}Ga-labeling at 100°C 44

VIII. References

1. Lieser, K. H. *Nuclear and Radiochemistry: Fundamentals and Applications: Lieser/Nuclear*. (Wiley-VCH Verlag GmbH, 1997). doi:10.1002/9783527612895.
2. Maxam, A. M. & Gilbert, W. A new method for sequencing DNA. *Proc. Natl. Acad. Sci. U.S.A.* **74**, 560–564 (1977).
3. Loosli, H. H., Lehmann, B. E. & Däppen, G. 4. Dating by Radionuclides. in *Studies in Environmental Science* vol. 43 153–174 (Elsevier, 1991).
4. Saha, G. B. *Basics of PET Imaging*. (Springer New York, 2010). doi:10.1007/978-1-4419-0805-6.
5. Jadvar, H. & Colletti, P. M. Competitive advantage of PET/MRI. *European Journal of Radiology* **83**, 84–94 (2014).
6. Antoch, G. *et al.* Non-small cell lung cancer: dual-modality PET/CT in preoperative staging. *Radiology* **229**, 526–533 (2003).
7. Wadsak, W. & Mitterhauser, M. Basics and principles of radiopharmaceuticals for PET/CT. *European Journal of Radiology* **73**, 461–469 (2010).
8. Gallagher, B. M. *et al.* Metabolic trapping as a principle of oradiopharmaceutical design: some factors resposible for the biodistribution of [18F] 2-deoxy-2-fluoro-D-glucose. *J. Nucl. Med.* **19**, 1154–1161 (1978).
9. Kulkarni, H. R. *et al.* Theranostics of prostate cancer: from molecular imaging to precision molecular radiotherapy targeting the prostate specific membrane antigen. *The British Journal of Radiology* 20180308 (2018) doi:10.1259/bjr.20180308.
10. Velikyan, I. Radionuclides for Imaging and Therapy in Oncology. in *Cancer Theranostics* 285–325 (Elsevier, 2014). doi:10.1016/B978-0-12-407722-5.00017-7.
11. Farwell, M. D., Pryma, D. A. & Mankoff, D. A. PET/CT imaging in cancer: current applications and future directions. *Cancer* **120**, 3433–3445 (2014).
12. de Paula Faria, D., Copray, S., Buchpiguel, C., Dierckx, R. & de Vries, E. PET imaging in multiple sclerosis. *Journal of Neuroimmune Pharmacology* **9**, 468–482 (2014).

13. Sarikaya, I. PET studies in epilepsy. *Am J Nucl Med Mol Imaging* **5**, 416–430 (2015).
14. Hirao, K. & Smith, G. S. Positron Emission Tomography Molecular Imaging in Late-Life Depression. *Journal of Geriatric Psychiatry and Neurology* **27**, 13–23 (2014).
15. Qayyum, A. A. & Kastrup, J. Measuring myocardial perfusion: the role of PET, MRI and CT. *Clin Radiol* **70**, 576–584 (2015).
16. Moerlein, S. M. & Welch, M. J. The chemistry of gallium and indium as related to radiopharmaceutical production. *International Journal of Nuclear Medicine and Biology* **8**, 277–287 (1981).
17. Moeller, Therald. & King, G. L. The Some Physicochemical Studies on Gallium(III) Salt Solutions. *The Journal of Physical and Colloid Chemistry* **54**, 999–1011 (1950).
18. Pearson, R. G. **Hard and Soft Acids and Bases**. *Journal of the American Chemical Society* **85**, 3533–3539 (1963).
19. Bandoli, G., Dolmella, A., Tisato, F., Porchia, M. & Refosco, F. Mononuclear six-coordinated Ga(III) complexes: A comprehensive survey. *Coordination Chemistry Reviews* **253**, 56–77 (2009).
20. Harris, W. R. & Pecoraro, V. L. Thermodynamic binding constants for gallium transferrin. *Biochemistry* **22**, 292–299 (1983).
21. Cherry, S. R., Sorenson, J. A. & Phelps, M. E. in *Physics in nuclear medicine* 43–53 (Elsevier/Saunders, 2012).
22. Holland, M. E., Deutsch, E. & Heineman, W. R. Studies on commercially available 99Mo/99mTc radionuclide generators—II. Operating characteristics and behavior of 99Mo/99mTc generators. *International Journal of Radiation Applications and Instrumentation. Part A. Applied Radiation and Isotopes* **37**, 173–180 (1986).
23. Gleason, G. I. A positron cow. *Int J Appl Radiat Isot* **8**, 90–94 (1960).
24. Yano, Y. & Anger, H. O. A GALLIUM-68 POSITRON COW FOR MEDICAL USE. *J. Nucl. Med.* **5**, 484–487 (1964).

25. Schuhmacher, J. & Maier-Borst, W. A new 68Ge/68Ga radioisotope generator system for production of 68Ga in dilute HCl. *The International Journal of Applied Radiation and Isotopes* **32**, 31–36 (1981).
26. Rosch, F. Reply: Impurity in 68Ga-Peptide Preparation Using Processed Generator Eluate. *Journal of Nuclear Medicine* **51**, 495–496 (2010).
27. Rosch, F. 68Ge/68Ga Generators and 68Ga Radiopharmaceutical Chemistry on Their Way into a New Century. *Journal of Postgraduate Medicine Education and Research* **47**, 18–25 (2013).
28. Breeman, W. A. P. *et al.* Radiolabelling DOTA-peptides with 68Ga. *European Journal of Nuclear Medicine and Molecular Imaging* **32**, 478–485 (2005).
29. Galema, S. A. Microwave chemistry. *Chemical Society Reviews* **26**, 233 (1997).
30. Elander, N., Jones, J. R., Lu, S.-Y. & Stone-Elander, S. Microwave-enhanced radiochemistry. *Chemical Society Reviews* **29**, 239–249 (2000).
31. Nüchter, M., Ondruschka, B., Bonrath, W. & Gum, A. Microwave assisted synthesis – a critical technology overview. *Green Chem.* **6**, 128–141 (2004).
32. Baghurst, D. R. & Mingos, D. M. P. Superheating effects associated with microwave dielectric heating. *Journal of the Chemical Society, Chemical Communications* 674 (1992) doi:10.1039/c39920000674.
33. Nüchter, M., Müller, U., Ondruschka, B., Tied, A. & Lautenschläger, W. Microwave-Assisted Chemical Reactions. *Chemical Engineering & Technology* **26**, 1207–1216 (2003).
34. Larhed, M., Olofsson, K. & Appukkuttan, P. *Microwave methods in organic synthesis*. (Springer, 2006).
35. Thorell, J.-O., Stone-Elander, S. & Elander, N. Use of a microwave cavity to reduce reaction times in radiolabelling with [11C]cyanide. *Journal of Labelled Compounds and Radiopharmaceuticals* **31**, 207–217 (1992).
36. Taylor, M. D., Roberts, A. D. & Nickles, R. J. Improving the yield of 2-[18F]fluoro-2-deoxyglucose using a microwave cavity. *Nucl. Med. Biol.* **23**, 605–609 (1996).

37. Velikyan, I., Beyer, G. J. & Långström, B. Microwave-Supported Preparation of ^{68}Ga Bioconjugates with High Specific Radioactivity. *Bioconjugate Chemistry* **15**, 554–560 (2004).
38. Velikyan, I. *et al.* Microwave accelerated68Ga-labelling of oligonucleotides. *Journal of Labelled Compounds and Radiopharmaceuticals* **47**, 79–89 (2004).
39. Alam, I. S. *et al.* Microwave gallium-68 radiochemistry for kinetically stable bis(thiosemicarbazone) complexes: structural investigations and cellular uptake under hypoxia. *Dalton Transactions* **45**, 144–155 (2016).
40. Audrain, H. Positron Emission Tomography (PET) and Microfluidic Devices: A Breakthrough on the Microscale? *Angewandte Chemie International Edition* **46**, 1772–1775 (2007).
41. Miller, P. W. Radiolabelling with short-lived PET (positron emission tomography) isotopes using microfluidic reactors. *Journal of Chemical Technology & Biotechnology* **84**, 309–315 (2009).
42. Rensch, C. *et al.* Microfluidics: A Groundbreaking Technology for PET Tracer Production? *Molecules* **18**, 7930–7956 (2013).
43. *Microfluidic devices for biomedical applications*. (Woodhead Publishing, 2013).
44. Pascali, G., Mazzone, G., Saccomanni, G., Manera, C. & Salvadori, P. A. Microfluidic approach for fast labeling optimization and dose-on-demand implementation. *Nuclear Medicine and Biology* **37**, 547–555 (2010).
45. Máté, G. *et al.* Multiparametric labeling optimization and synthesis of ^{68}Ga-labeled compounds applying a continuous-flow microfluidic methodology. *Journal of Flow Chemistry* **6**, 86–93 (2016).
46. Philippe, C. *et al.* [18F]FE@SNAP—A new PET tracer for the melanin concentrating hormone receptor 1 (MCHR1): Microfluidic and vessel-based approaches. *Bioorganic & Medicinal Chemistry* **20**, 5936–5940 (2012).
47. Ungersboeck, J. *et al.* Microfluidic preparation of [18F]FE@SUPPY and [18F]FE@SUPPY:2 — comparison with conventional radiosyntheses. *Nuclear Medicine and Biology* **38**, 427–434 (2011).

48. Pascali, G., Nannavecchia, G., Pitzianti, S. & Salvadori, P. A. Dose-on-demand of diverse 18F-fluorocholine derivatives through a two-step microfluidic approach. *Nucl. Med. Biol.* **38**, 637–644 (2011).
49. Selivanova, S. V. *et al.* Single-step radiofluorination of peptides using continuous flow microreactor. *Organic & Biomolecular Chemistry* **10**, 3871 (2012).
50. Pfaff, S. *et al.* Microfluidic ^{68} Ga-labeling: a proof of principle study. *Dalton Transactions* **47**, 5997–6004 (2018).
51. Berge, T. & Linell, F. Carcinoid tumours. Frequency in a defined population during a 12-year period. *Acta Pathol Microbiol Scand A* **84**, 322–330 (1976).
52. Ramage, J. K. *et al.* Guidelines for the management of gastroenteropancreatic neuroendocrine (including carcinoid) tumours (NETs). *Gut* **61**, 6–32 (2012).
53. Mizutani, G. *et al.* Expression of Somatostatin Receptor (SSTR) Subtypes (SSTR-1, 2A, 3, 4 and 5) in Neuroendocrine Tumors Using Real-time RT-PCR Method and Immunohistochemistry. *ACTA HISTOCHEMICA ET CYTOCHEMICA* **45**, 167–176 (2012).
54. Ambrosini, V., Fani, M., Fanti, S., Forrer, F. & Maecke, H. R. Radiopeptide imaging and therapy in Europe. *J. Nucl. Med.* **52 Suppl 2**, 42S-55S (2011).
55. Fani, M., Nicolas, G. P. & Wild, D. Somatostatin Receptor Antagonists for Imaging and Therapy. *J. Nucl. Med.* **58**, 61S-66S (2017).
56. Wild, D. *et al.* DOTA-NOC, a high-affinity ligand of somatostatin receptor subtypes 2, 3 and 5 for labelling with various radiometals. *Eur. J. Nucl. Med. Mol. Imaging* **30**, 1338–1347 (2003).
57. Wild, D. *et al.* 68Ga-DOTANOC: a first compound for PET imaging with high affinity for somatostatin receptor subtypes 2 and 5. *European Journal of Nuclear Medicine and Molecular Imaging* **32**, 724–724 (2005).
58. Wong, M. C. S. *et al.* Global Incidence and Mortality for Prostate Cancer: Analysis of Temporal Patterns and Trends in 36 Countries. *Eur. Urol.* **70**, 862–874 (2016).
59. *STATISTIK AUSTRIA, Österreichisches Krebsregister (Stand 06.12.2017)*.

60. Rojas, C., Frazier, S. T., Flanary, J. & Slusher, B. S. Kinetics and inhibition of glutamate carboxypeptidase II using a microplate assay. *Anal. Biochem.* **310**, 50–54 (2002).
61. Silver, D. A., Pellicer, I., Fair, W. R., Heston, W. D. & Cordon-Cardo, C. Prostate-specific membrane antigen expression in normal and malignant human tissues. *Clin. Cancer Res.* **3**, 81–85 (1997).
62. Eder, M. *et al.* Novel Preclinical and Radiopharmaceutical Aspects of [68Ga]Ga-PSMA-HBED-CC: A New PET Tracer for Imaging of Prostate Cancer. *Pharmaceuticals* **7**, 779–796 (2014).
63. Ray Banerjee, S. *et al.* Preclinical Comparative Study of ^{68} Ga-Labeled DOTA, NOTA, and HBED-CC Chelated Radiotracers for Targeting PSMA. *Bioconjugate Chemistry* **27**, 1447–1455 (2016).
64. Eder, M. *et al.* ^{68} Ga-Complex Lipophilicity and the Targeting Property of a Urea-Based PSMA Inhibitor for PET Imaging. *Bioconjugate Chemistry* **23**, 688–697 (2012).
65. Afshar-Oromieh, A. *et al.* Comparison of PET imaging with a 68Ga-labelled PSMA ligand and 18F-choline-based PET/CT for the diagnosis of recurrent prostate cancer. *European Journal of Nuclear Medicine and Molecular Imaging* **41**, 11–20 (2014).
66. Langer, H. F., Haubner, R., Pichler, B. J. & Gawaz, M. Radionuclide imaging: a molecular key to the atherosclerotic plaque. *J. Am. Coll. Cardiol.* **52**, 1–12 (2008).
67. Szekanecz, Z., Besenyei, T., Szentpétery, A. & Koch, A. E. Angiogenesis and vasculogenesis in rheumatoid arthritis. *Curr Opin Rheumatol* **22**, 299–306 (2010).
68. Sheppard, D. Endothelial integrins and angiogenesis: not so simple anymore. *J. Clin. Invest.* **110**, 913–914 (2002).
69. Ruoslahti, E. & Pierschbacher, M. D. New perspectives in cell adhesion: RGD and integrins. *Science* **238**, 491–497 (1987).
70. Giancotti, F. G. Integrin Signaling. *Science* **285**, 1028–1033 (1999).
71. Sheldrake, H. M. & Patterson, L. H. Function and antagonism of beta3 integrins in the development of cancer therapy. *Curr Cancer Drug Targets* **9**, 519–540 (2009).
72. Haubner, R. *et al.* Radiolabeled alpha(v)beta3 integrin antagonists: a new class of tracers for tumor targeting. *J. Nucl. Med.* **40**, 1061–1071 (1999).

73. Haubner, R. *et al.* [18F]Galacto-RGD: synthesis, radiolabeling, metabolic stability, and radiation dose estimates. *Bioconjug. Chem.* **15**, 61–69 (2004).

74. Decristoforo, C. *et al.* 68Ga- and 111In-labelled DOTA-RGD peptides for imaging of alphavbeta3 integrin expression. *Eur. J. Nucl. Med. Mol. Imaging* **35**, 1507–1515 (2008).

75. Sun, Y. *et al.* Indium (III) and gallium (III) complexes of bis(aminoethanethiol) ligands with different denticities: stabilities, molecular modeling, and in vivo behavior. *J. Med. Chem.* **39**, 458–470 (1996).

76. Knetsch, P. A. *et al.* [68Ga]NODAGA-RGD for imaging αvβ3 integrin expression. *European Journal of Nuclear Medicine and Molecular Imaging* **38**, 1303–1312 (2011).

77. Meyer, G.-J., Mäcke, H., Schuhmacher, J., Knapp, W. H. & Hofmann, M. 68Ga-labelled DOTA-derivatised peptide ligands. *European Journal of Nuclear Medicine and Molecular Imaging* **31**, (2004).

78. Mukherjee, A., Pandey, U., Chakravarty, R., Sarma, H. D. & Dash, A. Development of Single Vial Kits for Preparation of 68Ga-Labelled Peptides for PET Imaging of Neuroendocrine Tumours. *Molecular Imaging and Biology* **16**, 550–557 (2014).

79. Garcia-Arguello, S. F., Lopez-Lorenzo, B. & Ruiz-Cruces, R. Automated production of [^{68} Ga]Ga-DOTANOC and [^{68} Ga]Ga-PSMA-11 using a TRACERlab FX $_{FN}$ synthesis module. *Journal of Labelled Compounds and Radiopharmaceuticals* **62**, 146–153 (2019).

80. Yagi, Y. *et al.* Efficient gallium-68 radiolabeling reaction of DOTA derivatives using a resonant-type microwave reactor. *Journal of Labelled Compounds and Radiopharmaceuticals* **62**, 132–138 (2019).

81. Ebenhan, T. *et al.* Development of a Single Vial Kit Solution for Radiolabeling of 68Ga-DKFZ-PSMA-11 and Its Performance in Prostate Cancer Patients. *Molecules* **20**, 14860–14878 (2015).

82. Bauwens, M., Chekol, R., Vanbilloen, H., Bormans, G. & Verbruggen, A. Optimal buffer choice of the radiosynthesis of (68)Ga-Dotatoc for clinical application. *Nucl Med Commun* **31**, 753–758 (2010).

83. Velikyan, I., Beyer, G. J. & Långström, B. Microwave-Supported Preparation of ^{68}Ga Bioconjugates with High Specific Radioactivity. *Bioconjugate Chemistry* **15**, 554–560 (2004).